

# Recent Advances in Photovoltaic and Photovoltaic Thermal Technologies of Integrated Phase-Change Materials: A Review

Manting Fang, Xuelai Zhang,\* Yang Liu, and Shaowei Cai

**Photovoltaic (PV) cells convert solar energy into electricity is currently the cleanest and most economical way to generate electricity. Nevertheless, just a portion of the solar power can be transformed into electrical energy, while the remaining portion is converted into heat, leading to an increase in the temperature of the PV cells. The rise in temperature will not only cause a decrease in the electrical efficiency of PV cells, but it may also impact their life span. By placing phase-change materials (PCMs) on the back of the PV cells, it is possible to decrease the temperature increase and enhance the electrical efficiency. The heat collected by PCMs can also be taken away using liquid cooling and put to use. In this article, the classification, performance evaluation, and composite modification technology of PCMs are introduced in detail. The practical application requirements of PCMs in thermal management of PV cells are discussed, and some new ideas of applying PCMs to PV cells are prospected. Moreover, the prior investigations regarding the incorporation of PCMs with PV systems and PV/T systems are also compiled, encompassing the various research perspectives and methodologies employed. In addition, the possible development direction in the future is prospected.**

## 1. Introduction

Energy and environment are two major key issues in the 21st century.<sup>[1]</sup> Energy is the essential foundation for the existence and progress of humanity. As the population grows and people's living conditions improve, the need for energy is steadily rising. The 2017 World Energy Outlook Report predicts a 30% rise in global energy demand from 2017 to 2040.<sup>[2]</sup> Therefore, the development and utilization of energy is facing both opportunities and challenges. Excessive utilization of fossil fuels like coal, petroleum, and gas will result in pollution of the environment, deterioration of the climate, and destruction of ecosystems. Energy conservation and environmental protection are two important tasks that the world must complete.<sup>[3]</sup>

---

M. Fang, X. Zhang, Y. Liu, S. Cai  
Merchant Marine College  
Shanghai Maritime University  
Shanghai 201306, China  
E-mail: xlzhang@shmtu.edu.cn

 The ORCID identification number(s) for the author(s) of this article can be found under <https://doi.org/10.1002/solr.202400033>.

DOI: 10.1002/solr.202400033

The global rollout of the two-carbon strategy has sparked great interest in the development and utilization of renewable energy sources. Solar energy, which possesses energy reserves that are not only limitless but also emits no pollutants when utilized, offers effective solutions to existing energy and environmental challenges. However, the intermittent and unpredictable nature of solar energy limits its practical application.<sup>[4]</sup> Thermal energy storage technology allows for the storage of surplus solar energy during periods of abundant sunlight, which can then be released during times of insufficient visible light, such as nights or cloudy days. By utilizing thermal energy storage technology, it is possible to directly store the heat produced by solar radiation, resulting in optimal efficiency. Thermal energy storage technology can be divided into three categories: sensible heat thermal energy storage, latent heat thermal energy storage (LHTES), and thermochemical thermal energy storage.<sup>[5]</sup>

Compared with sensible heat storage and chemical heat storage, LHTES has attracted more attention due to its small size, strong heat storage capacity, and temperature control ability.<sup>[6]</sup>

The core of LHTES is phase-change materials (PCMs).<sup>[7]</sup> The excellent properties of PCMs, including their high latent heat and almost constant temperature throughout the phase change, bring many benefits to LHTES. Inorganic PCMs, for instance, exhibit deficiencies like supercooling and phase separation, while organic PCMs suffer from disadvantages such as low thermal conductivity and a slightly higher cost.<sup>[8]</sup> As a result of these shortcomings, PCMs can only be utilized following composite alteration, and unmodified pure PCMs lack any practical utility.<sup>[9]</sup> Therefore, PCMs have received the attention of many researchers.

At present, the application of solar energy can be roughly divided into two categories: one is the use of solar collectors to collect and use the heat generated by sunlight, and the other is the use of photovoltaic (PV) cells to generate electricity.<sup>[10]</sup> Despite solar heat collection being developed earlier than PV systems, the latter are now more widely utilized due to their ability to generate clean electricity.

In actual work, PV cells are prone to decrease electrical efficiency due to high temperature with direct sunlight irradiation<sup>[11]</sup>—a phenomenon that will be introduced in more detail in Section 3. Placing PCMs on the rear side of PV cells can

decelerate the increase in temperature of PV cells, thereby enhancing the efficiency of power generation in PV systems. Systems consisting of PV cells and PCMs are called PV–PCM systems.<sup>[12]</sup> As a passive temperature control technology, PCMs cooling only requires low cost and energy consumption compared to active cooling, providing better temperature uniformity. However, it has lower cooling efficiency than active liquid cooling and lacks the flexibility of active cooling.<sup>[13]</sup> When PV–PCM systems are paired with liquid cooling, the liquid working medium (such as water or nanofluids) will extract and utilize the heat energy collected by the PCMs, resulting in the formation of PV/T-PCM systems.<sup>[14]</sup> PV/T-PCM systems have gained momentum in recent years because of their ability to combine active and passive cooling methods while also optimizing energy use. This field is becoming a research focus.

The application potential of PCMs in PV systems and PV/T systems is significant, making it crucial to summarize and discuss the related researches. Therefore, this article begins with an introduction to LHTES technology and provides a comprehensive overview of PCMs classification, performance testing, and composite modification techniques. The practical application requirements of PCMs behind PV cells are summarized, and the new ideas of PCMs modification applied to PV cells are prospected. Then, in Section 3 and 4, the integration of PCMs in PV systems and PV/T systems is summarized, covering various research perspectives and methods. The key points and shortcomings of the existing research are also summarized and the future development direction is prospected.

## 2. PCMs and LHTES Technology

### 2.1. Introduction to LHTES

LHTES technology is realized by using PCMs to absorb or release a large amount of latent heat during the phase-change process.<sup>[15]</sup> There are four forms of phase changes of matter: gas–solid, gas–liquid, liquid–solid, and solid–solid.<sup>[16]</sup> The volume variations during solid–gas and liquid–gas phase change in the mentioned four forms are excessively significant and challenging to manage. Additionally, the latent heat associated with solid–solid phase change is frequently less than that of solid–liquid phase change. Therefore, the solid–liquid phase change is the most suitable for practical application. PCMs are often referred to directly as solid–liquid PCMs.<sup>[17]</sup> During practical use, when the surrounding temperature surpasses the melting point of PCMs, PCMs undergo a phase change and assimilate thermal energy, thereby initiating the heat storage procedure. If the ambient temperature drops below the freezing point of the PCMs, the PCMs will solidify and release heat, thus carrying out the exothermic process. Therefore, the heat energy stored by LHTES is composed of sensible heat before and after phase change and latent heat during phase change, as shown in Equation (1).<sup>[18]</sup>

$$Q = \int_{T_1}^T mC_{p,m} dT + m\Delta H_m + \int_T^{T_2} mC_{p,m} dT \quad (1)$$

In Equation (1),  $Q$  represents the amount of heat stored, while  $m$  stands for PCM's mass;  $C_{p,m}$  denotes the specific heat capacity

of the PCM and  $\Delta H_m$  represents its melting enthalpy; and  $T_1$  and  $T_2$  indicate the initial and final temperatures of the PCM during the heat storage process, respectively, while  $T$  signifies the PCM's phase-change temperature.

PCMs are the foundation of LHTES. Therefore, to make LHTES compatible with PV cells, it is necessary to first prepare PCMs that meet the requirements of use and have good performance.

### 2.2. Classification and Characteristics of PCMs

There are three types of PCMs: organic PCMs, inorganic PCMs, and eutectic PCMs.<sup>[7]</sup> Figure 1 illustrates the categorization of PCMs. Paraffin is the most common type of organic PCMs. In addition to this broad category, organic PCMs also include alcohols and fatty acids. Inorganic PCMs encompass hydrated salts, molten salts, and metals. Compared with molten salts and metals, the phase-change temperature of hydrated salts PCMs is more suitable for room temperature. Therefore, hydrated salt PCMs become the most widely used inorganic PCMs. Eutectic PCMs are prepared by two or more PCMs using the melt blending method. If the phase-change temperature of a single kind of PCM is inconsistent with the current working conditions, eutectic PCMs can be synthesized to meet the needs. The phase-change temperature and latent heat of the obtained eutectic PCMs are lower than that of either component.<sup>[19]</sup>

Organic PCMs, inorganic PCMs, and eutectic PCMs each have unique advantages in their applications due to their different physical and chemical properties, prices, and other factors. Organic PCMs offer the benefits of minimal supercooling and no phase separation, but they also have drawbacks such as lower thermal conductivity and latent heat. Despite the fact that inorganic PCMs typically have higher thermal conductivity and latent heat compared to organic PCMs, they still face challenges such as significant supercooling and phase separation. Eutectic PCMs can achieve suitable phase-change temperature, but their latent heat is lower than that of any component.<sup>[20]</sup> Table 1 summarizes

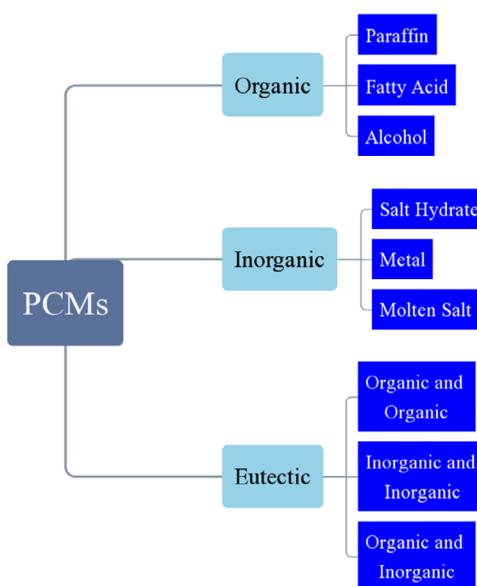


Figure 1. Categorization of PCMs.

**Table 1.** Advantages and disadvantages of different types of PCMs.

Type of PCMs	Advantages	Disadvantages
Organic PCMs	Low supercooling	Lower thermal conductivity
	No phase separation	Combustible
	Less impact on the environment	Higher price Perishable
Inorganic PCMs	High latent heat	High supercooling
	Higher thermal conductivity	Phase separation problem
	Low price, easy access	Poor cyclic stability
	Recyclable Nonflammable	Corrosive to metal containers
Eutectic PCMs	Suitable phase-change temperature	Low latent heat

the advantages and disadvantages of organic, inorganic, and eutectic PCMs.

The use of organic, inorganic, and eutectic PCM involves different properties, and each PCMs species has its own set of advantages and disadvantages. Hence, it is crucial to conduct performance testing and composite modification of PCMs during their development. These two important processes are described later.

### 2.3. Performance Test of PCMs

Special experimental equipment and methods are required to test the phase-change temperature, latent heat value, and thermal conductivity, which are significant performance parameters of PCMs. In addition to performance parameters, PCMs also need to meet some important properties, such as good thermal and chemical stability. It is also important to test whether PCMs meet these properties.

#### 2.3.1. Phase-Change Temperature and Latent Heat

Differential scanning calorimetry (DSC) has been widely utilized in previous research to identify the phase-change temperature and latent heat of PCMs.<sup>[21]</sup> The DSC technique offers the benefits of exceptional effectiveness and precision, enabling the precise determination of phase-change temperature and latent heat of the PCMs within a short span of tens of minutes. The DSC method only requires a small quantity of PCM samples, whereas the mass of PCMs is strongly linked to the phase-change temperature and latent heat of PCMs. Hence, the DSC test findings may not accurately reflect the true characteristics of numerous samples.<sup>[22]</sup>

Zhang et al.<sup>[23]</sup> developed the T-history technique. A vast number of samples' phase-change temperature and latent heat can be rapidly acquired. This method can also test multiple PCMs samples simultaneously, which improves efficiency. The experimental equipment required by T-history method is simple and the price is much lower than that of a DSC. Nevertheless, the utilization rate of the T-history technique in scientific investigations is considerably lower compared to that of DSC, primarily due to

the necessity for further examination of its applicability and the need for enhancing result precision.<sup>[24]</sup>

#### 2.3.2. Thermal Conductivity

There are two main methods for measuring thermal conductivity: the steady-state method and the transient method.<sup>[25]</sup> In comparison to the steady-state technique, the transient approach offers not only a reduced measurement time but also the ability to measure a significantly broader range of sample thicknesses than the steady-state method.<sup>[26]</sup> Hence, the transient technique is commonly employed in scientific studies to determine the thermal conductivity of PCMs. Methods for transient analysis encompass the transient hot-wire method, the transient plane heat source method, the laser method, and the periodic heat flow method.<sup>[27]</sup>

By inserting a heated wire into a sample, applying an electric current to the wire or changing the temperature of the sample, the thermal conductivity, thermal diffusion coefficient, and other parameters of the sample can be obtained through computer data processing. The aforementioned measurement method is the transient hot-wire method. The transient hot-wire method does not impose any specific conditions on the sample's shape, leading to an imbalanced heat transfer in all directions within the sample, consequently impacting the measurement outcomes.<sup>[28]</sup> To achieve a full balance of temperature changes, the PCMs sample can be transformed into a disk shape by grinding or cutting. This method is known as the transient plane heat source method and serves as the foundation for the hot-disk thermal constant analyzer. The hot-disk thermal constant analyzer is unable to provide accurate measurements of thermal conductivity for transparent or translucent materials due to the potential impact of thermal radiation within the materials on the results of the measurement.<sup>[29]</sup>

The laser method and the periodic heat flow method first measure the thermal diffusion coefficient and specific heat of PCM at a specific temperature. Then, the thermal conductivity of PCM is calculated by multiplying the thermal diffusion coefficient and specific heat with the PCM density at this temperature.<sup>[30]</sup> Scientific research institutions have adopted the laser method as the dominant approach for testing thermal conductivity due to its rapid and efficient nature, as well as its superior measurement precision compared to the hot-disk thermal constant analyzer.

#### 2.3.3. Supercooling Degree

The extensive supercooling degree restricts the utilization of hydrated salt PCMs, and assessing the supercooling level of these PCMs is a crucial step in the development of hydrated salt composite PCMs.

To determine the supercooling degree of hydrated salt PCMs, the cooling solidification process of molten PCMs must be monitored in real time. Temperature measuring devices such as thermocouples and data acquisition instruments are used here to record temperature changes in real time. The curve obtained in this way is called cooling curve. Figure 2<sup>[31]</sup> shows a representative diagram of the cooling experimental system. To determine

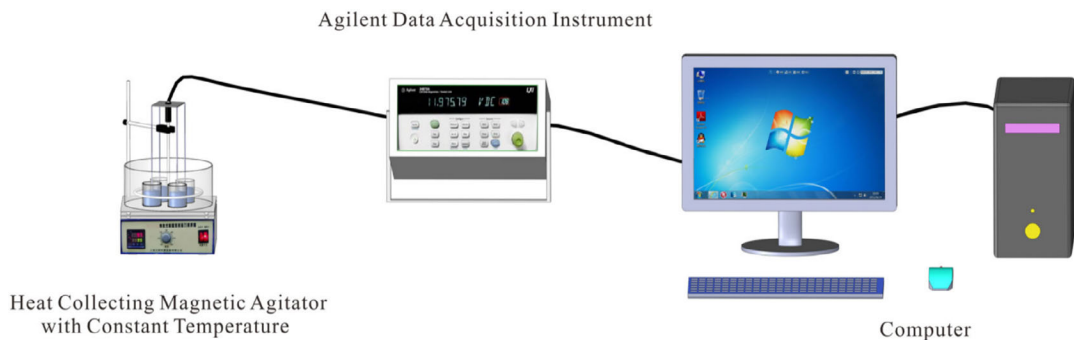


**Figure 2.** Diagram of cooling experimental system.

the supercooling degree of PCMs, the temperature at which the PCMs begin to crystallize in the cooling curve can be compared with the phase-change temperature measured by DSC. **Table 2** summarizes the supercooling degree of pure hydrated salts PCMs.

#### 2.3.4. Thermal Stability and Composition Analysis

PCMs need to have good thermal stability at the operating temperature, and neither PCMs nor its additives can be degraded. To assess the thermal stability of PCMs, one can use a thermogravimetric analyzer to measure the mass variation of PCMs at specific temperatures.<sup>[32]</sup>

Eutectic PCMs are obtained by melting and blending two kinds of PCMs according to a certain proportion. Analysis of the chemical composition of eutectic PCMs is essential to verify that no chemical reactions are present during preparation. X-ray diffraction (XRD) and Fourier transform infrared (FT-IR) spectroscopy<sup>[33]</sup> are the instruments often used in this case. The test ideas using these two instruments are different. XRD detects the crystal structure of each component in the eutectic PCMs and compares it with the eutectic PCMs to determine if new substances are present. FT-IR determines the formation of new substances by checking for the presence of new chemical bonds between the subcomponents and eutectic PCMs.<sup>[34]</sup> In addition, the composition of PCMs can be microscopically investigated using scanning electron microscopy (SEM) to determine whether

PCMs and additives are effectively integrated in composite PCMs.

#### 2.4. Composite Modification of PCMs

In this section, the utilization of additives to enhance the heat storage performance of PCMs through compound modification is explained.

##### 2.4.1. Supercooling Degree

Table 2 shows that many hydrated salt PCMs do not crystallize naturally and cannot be utilized due to the very high supercooling degree. Therefore, it is necessary to take measures to reduce or even eliminate the supercooling degree so that the hydrated salt PCMs can effectively release heat at the target temperature.<sup>[35]</sup>

The nucleation crystallization of PCMs requires a driving force, and the supercooling is the manifestation of this driving force. Substances that can provide driving force for the crystallization of PCMs are called nucleating agents.<sup>[36]</sup> To decrease the supercooling degree of hydrated salt PCMs, the most efficient and cost-effective approach is the incorporation of nucleating agents. There are three categories in which nucleating agents can be classified. Class (a) nucleating agents have similar structure to PCM, which can stimulate the nucleation of PCM. Both  $\text{Na}_2\text{HPO}_4 \cdot 12\text{H}_2\text{O}$  and  $\text{CH}_3\text{COONa} \cdot 3\text{H}_2\text{O}$  solution systems contain  $\text{Na}^+$  ions, making  $\text{Na}_2\text{HPO}_4 \cdot 12\text{H}_2\text{O}$  a suitable choice as a nucleating agent for  $\text{CH}_3\text{COONa} \cdot 3\text{H}_2\text{O}$  PCM. The addition of  $\text{Na}_2\text{HPO}_4 \cdot 12\text{H}_2\text{O}$  can reduce the supercooling degree of  $\text{CH}_3\text{COONa} \cdot 3\text{H}_2\text{O}$  to 0.5 °C.<sup>[37]</sup> Class (b) nucleating agents have no similar structure to PCM, but its lattice surface provides a preferred deposition position for PCM to promote the crystallization of PCM. As an illustration, CaF can serve as a nucleation promoter to decrease the extent of supercooling of  $\text{Ba}(\text{OH})_2 \cdot 8\text{H}_2\text{O}$  to 1.8 °C.<sup>[38]</sup> Class (c) nucleating agents are some high thermal conductivity materials, among which nanomaterials are typical. Their addition improves the heat transfer performance and crystallization degree of hydrated salt PCMs.<sup>[39]</sup>

There are two methods to find suitable nucleating agents for PCMs, one is the “Scientific Method” and the other is the “Edison Method”.<sup>[40]</sup> The “Scientific Method” is to find substances with similar lattice parameters to PCMs in the crystal data table as candidate nucleating agents, and then select the truly

**Table 2.** Supercooling degree of pure hydrated salts PCMs.

PCM	Supercooling degree [°C]	Reference
$\text{CaCl}_2 \cdot 6\text{H}_2\text{O}$	25.2	[127]
$\text{Na}_2\text{SO}_4 \cdot 10\text{H}_2\text{O}$	27.31	[128]
$\text{Zn}(\text{NO}_3)_2 \cdot 6\text{H}_2\text{O}$	Greater than 12	[129]
$\text{Na}_2\text{HPO}_4 \cdot 12\text{H}_2\text{O}$	18.4	[130]
$\text{CH}_3\text{COONa} \cdot 3\text{H}_2\text{O}$	Greater than 58.3	[131]
$\text{Ba}(\text{OH})_2 \cdot 8\text{H}_2\text{O}$	13	[132]
$\text{Mg}(\text{NO}_3)_2 \cdot 6\text{H}_2\text{O}$	25.05	[133]
$\text{KAl}(\text{SO}_4)_2 \cdot 12\text{H}_2\text{O}$	19.4	[134]
$\text{MgCl}_2 \cdot 6\text{H}_2\text{O}$	40.6	[135]

**Table 3.** Nucleating agents suitable for frequently used hydrated salts PCMs.

PCM	Nucleating agent	Supercooling degree after modification [°C]	Reference
CaCl <sub>2</sub> ·6H <sub>2</sub> O	SrCl <sub>2</sub> ·6H <sub>2</sub> O	0.39	[136]
Na <sub>2</sub> SO <sub>4</sub> ·10H <sub>2</sub> O	Na <sub>2</sub> B <sub>4</sub> O <sub>7</sub> ·10H <sub>2</sub> O	Less than 2	[137]
Zn(NO <sub>3</sub> ) <sub>2</sub> ·6H <sub>2</sub> O	ZnO	2.6	[129]
Na <sub>2</sub> HPO <sub>4</sub> ·12H <sub>2</sub> O	Na <sub>4</sub> P <sub>2</sub> O <sub>7</sub> ·10H <sub>2</sub> O	1.3	[138]
CH <sub>3</sub> COONa·3H <sub>2</sub> O	Na <sub>2</sub> HPO <sub>4</sub> ·12H <sub>2</sub> O	0.5	[37]
Ba(OH) <sub>2</sub> ·8H <sub>2</sub> O	CaF	Less than 1	[38]
Mg(NO <sub>3</sub> ) <sub>2</sub> ·6H <sub>2</sub> O	Carbon sphere	6.3	[139]
KAl(SO <sub>4</sub> ) <sub>2</sub> ·12H <sub>2</sub> O	Na <sub>2</sub> B <sub>4</sub> O <sub>7</sub> ·10H <sub>2</sub> O	0.794	[140]
MgCl <sub>2</sub> ·6H <sub>2</sub> O	Sr(OH) <sub>2</sub>	0.1	[141]

effective nucleating agents through experimental verification. Despite having a specific theoretical basis, unfortunately not all nucleating agents have a crystal structure similar to that of PCMs. The “Edison Method” is a more efficient method, but requires less brain power. The “Edison Method” depends on the researcher’s personal intuition to choose a vast array of substances for experimentation to discover nucleating agents. The quantity of nucleating agents discovered through this approach surpasses that of the “Scientific Method”. Although there is no perfect method to find nucleating agents until now, related studies have been frequent in the past 20 years. So far, scientists have found nucleating agents suitable for frequently used hydrated salts PCMs, as shown in **Table 3**.

The issue of supercooling of hydrated salt eutectic PCMs has emerged as a recent area of focus. Hydrated salt eutectic PCMs consists of two or more hydrated salts. If these inorganic hydrated salts do not promote nucleation with each other, the supercooling of the hydrated salt eutectic PCM may be greater than the supercooling of either component. In this case, the effective nucleating agent of one component of the eutectic PCM may not reduce the degree of supercooling of the eutectic PCM. Therefore, additional tests must be performed to identify nucleating agents that are equally effective against eutectic PCM.<sup>[41]</sup> The aforementioned are the ideas and methods of finding eutectic PCMs’ nucleating agents. Compared with the search method of nucleating agent in single-component hydrated salt PCMs, this method is more effective than “Edison Method” and more reasonable than “Scientific Method”.

#### 2.4.2. Phase Separation

Phase separation is a significant obstacle that hinders the practical use of inorganic hydrated salt PCMs. This issue is determined by the molten state’s homogeneous stability of hydrated salt PCMs. The reasons for phase separation of single hydrated salt and eutectic hydrated salt are different. Hydrated salts are stable hydrated salts and unstable hydrated salts.<sup>[42]</sup> Unstable hydrated salts lose their crystalline water when they melt, forming hydrated salts with less crystalline water or completely dehydrated inorganic salts. A precipitate will form if the newly generated substance is insoluble in the system. Following the

**Table 4.** Classification of thickeners.

Thickener classification	Natural polymer	Synthetic polymer	Cellulose thickener	Inorganic thickener
Thickener	Xanthan gum	Sodium polyacrylate	Carboxymethylcellulose sodium	Attapulgite clay
	Guar gum	Polyacrylamide	Methylcellulose	Diatomite
	Sodium alginate		Hydroxyethyl cellulose (HEC)	(SA)

cooling procedure, PCMs are separated into three distinct layers: the top layer consists of a solution, the middle layer comprises a hydrated salt, and the bottom layer is composed of an insoluble precipitate.<sup>[43]</sup>

The reason for the separation of single hydrated salt PCMs is as mentioned earlier. To address the issue of phase separation, there are two possible approaches: 1) incorporating a thickening agent and 2) employing porous materials for adsorption.<sup>[44]</sup>

Most thickeners are soluble in water. Due to their unique composition, they exhibit high viscosity in aqueous solutions, which hinders the settling of particles and thus solves the phase separation problem of hydrated salts.<sup>[45]</sup> Thickeners commonly used to solve the separation of hydrated salt phases can be divided into four categories according to their material structure, as shown in **Table 4**. However, the thickeners mentioned in the table may not be suitable for all types of hydrated salts and need to be experimentally tested. Therefore, it is necessary to further study the thickening mechanism of thickener and the effect of improving phase separation. This will help simplify the experimental procedures for verifying the suitability of the thickener. The porous materials have sufficient interconnected pores and large surface area to ensure the effective absorption of PCMs in the pores. Consequently, this resolves the issue of phase separation in hydrated salt PCMs.<sup>[46]</sup> The PCMs thus prepared are called shape-stabilized composite PCMs.<sup>[47]</sup> Commonly used porous materials include carbon, mineral, and metallic porous materials,<sup>[48]</sup> as shown in **Figure 3**. Porous materials also provide an important way to encapsulate PCMs, ensuring that PCMs do not leak.<sup>[49]</sup> It should be noted that for PCMs experiencing significant phase separation, like Na<sub>2</sub>SO<sub>4</sub>·10H<sub>2</sub>O, thickeners or porous adsorption alone are often inadequate, and additional research is required to address the phase separation of these PCMs.

The delamination of eutectic PCMs in their molten state, similar to a cocktail, occurs due to the disparity in density between two or more hydrated salts. The naked eyes are often unable to observe this phenomenon of phase separation, but it can only be detected through DSC detection or SEM observation, leading to a lack of further study on it.

#### 2.4.3. Thermal Conductivity

PCMs typically exhibit low thermal conductivity. Although the thermal conductivity of inorganic PCMs is better than that of organic PCMs, there is still a significant gap with the practical application requirements.<sup>[50]</sup> To utilize PCMs in PV cells,

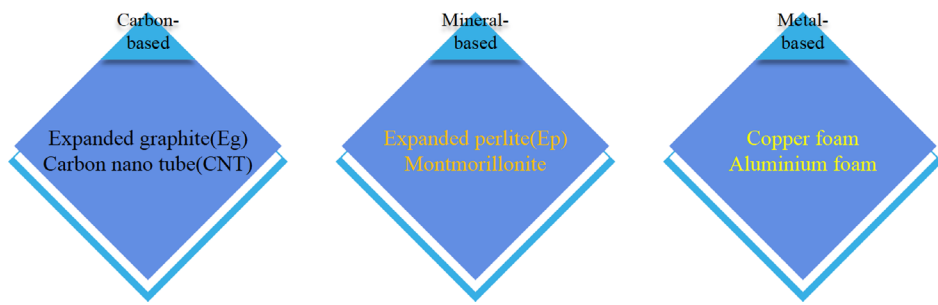


**Figure 3.** Classification of porous materials.

enhancing the thermal conductivity of PCMs is imperative. Thermal conductivity enhancers can be categorized into 0D structure additives, 1D structure additives, 2D structure additives, and 3D structure additives.<sup>[51]</sup> Among them, 0D, 1D, 2D, and 3D represent the shape characteristics of the thermal conductivity path generated by the additive: 0D means that the heat conduction path is composed of points; 1D means that the heat conduction path is made up of lines; 2D means that the heat conduction path is composed of surfaces; and 3D means that the heat conduction paths are interconnected and thus become a whole.

**0D Structure Additives:** Nanoparticle materials serve as the representatives of 0D structure additives.<sup>[52]</sup> Nanoparticle materials not only enhance the thermal conductivity of PCMs, but also reduce the supercooling degree of PCMs, so it has received great attention. Nanoparticle materials have advantages such as considerable surface area, strong interfacial interaction, commendable uniformity, and dispersion.<sup>[53]</sup> Commonly used

nanoadditive additives include nano-Cu, nano-Al<sub>2</sub>O<sub>3</sub>, nano-CuO, nano-TiO<sub>2</sub>, nano-Fe<sub>2</sub>O<sub>3</sub>, and nano-ZnO, etc.<sup>[54]</sup> **Table 5** summarizes the enhancement impact of incorporating nanoparticle materials on the thermal conductivity of PCMs.

**1D Structure Additives:** Carbon-based materials like graphene, carbon nanotubes (CNTs), and graphite are among the 1D structure additives.<sup>[55]</sup> The 1D structure additives have good thermal conductivity, light weight, and minimal influence on the latent heat value of PCMs.<sup>[56]</sup> **Table 6** summarizes the impact of incorporating 1D structural additives on the thermal conductivity of PCMs.

**2D Structure Additives:** The 2D structure additives include carbon-based polyporous materials and mineral-based polyporous materials<sup>[57]</sup> mentioned in Section 2.4.2. The presence of a large number of pores and surface areas in these permeable substances not only improves the thermal conductivity of PCMs, but also prevents potential liquid-phase leakage of PCMs. **Table 7** summarizes the impact of incorporating 2D structure additives on the thermal conductivity of PCM.

**Table 5.** The 0D structure additives.

0D structure additive	PCM	Additive proportion	Effect [W m <sup>-1</sup> K <sup>-1</sup> ]	Reference
Nano-Cu	Zn(NO <sub>3</sub> ) <sub>2</sub> ·6H <sub>2</sub> O	0.5 wt%	0.4 → 0.63	[142]
	Polyethylene glycol (PEG)	3 wt%	0.235 → 0.281	[143]
	Lauric acid (LA)	2 wt%	0.16 → 0.33	[144]
Nano-Al <sub>2</sub> O <sub>3</sub>	PEG	3 wt%	0.297 → 0.435	[145]
	Myristic acid (MA) + high density polyethylene	12 wt%	0.2038 → 0.3972	[146]
	Na <sub>2</sub> SO <sub>4</sub> ·10H <sub>2</sub> O–Na <sub>2</sub> HPO <sub>4</sub> ·12H <sub>2</sub> O	4.55 wt%	0.789 → 1.278	[147]
Nano-CuO	Neopentyl glycol (NPG)	0.1 wt%	0.109 → 0.125	[148]
	Candle making wax (CMW)	2 vol%	0.17 → 0.242	[149]
	Paraffin	1 vol%	0.18 → 0.228	[150]
Nano-TiO <sub>2</sub>	LA + stearic acid (SA)	1 wt%	0.19 → 0.27	[151]
	Paraffin	3 wt%	0.147 → 0.195	[152]
	CaCl <sub>2</sub> ·6H <sub>2</sub> O–MgCl <sub>2</sub> ·6H <sub>2</sub> O	0.5 wt%	0.552 → 0.828	[153]
Nano-Fe <sub>2</sub> O <sub>3</sub>	Paraffin wax	10 wt%	0.25 → 0.37	[154]
	Beeswax	4 wt%	0.25 → 0.272	[155]
Nano-ZnO	Crude wax	1 wt%	0.18 → 0.23	[156]

**Table 6.** The 1D structure additives.

1D structure additive	PCM	Additive proportion [wt%]	Effect [W m <sup>-1</sup> K <sup>-1</sup> ]	Reference
Graphene	Beeswax	0.25	0.25 → 2.89	[157]
	Tetradecanol	10	0.221 → 1.031	[158]
	CNTs	Palmitic acid (PA)	1	0.22 → 0.33
Graphite	n-Eicosane	1	0.22 → 0.32	[160]
	Paraffin	5.27	0.204 → 0.516	[161]
	Polyethylene	20	0.51 → 1.31	[162]
Paraffin	Paraffin	8	0.27 → 0.51	[163]
	SA	5	0.1255 → 0.4043	[164]

**Table 7.** The 2D structure additives.

2D structure additive	PCM	Additive proportion [wt%]	Effect [W m <sup>-1</sup> K <sup>-1</sup> ]	Reference
Expanded graphite (EG)	Pentaglycerine	4	0.232 → 0.944	[165]
	SA-benzamide	16	0.3396 → 5.381	[166]
Bentonite	MA	50	0.17 → 0.32	[167]

**3D Structure Additives:** The 3D structure additives include metal foam, graphite foam, and 3D network carbon;<sup>[58]</sup> they can form a network of interconnected pores, providing more pathways for heat transfer in PCMs.<sup>[59]</sup> Since the main preparation methods are vacuum impregnation or solution casting, there is a lack of literature discussing the ratio of 3D structural additives/PCMs. Consequently, this article does not include a summary of the 3D structure additives in the table.

#### 2.4.4. Cycle Stability

In practical applications, PCMs have to go through thousands or even tens of thousands of melt-solidification cycles.<sup>[60]</sup> In the course of multiple cycles, PCMs are very likely to undergo denaturation. Denaturation can reduce the heat storage performance of PCMs.<sup>[61]</sup> The denaturation mechanism varies between inorganic and organic PCMs. The denaturation of hydrated salt PCMs is mainly due to the loss of crystal water, while the denaturation of organic PCMs is mainly caused by chemical factors such as oxidation.<sup>[62]</sup> Denaturation limits the long-term use of PCMs. To enhance the durability of PCMs, the required substances are identical to those used for addressing phase separation. However, the methods employed, such as incorporating thickeners and porous materials, differ in their underlying principles. Taking hydrated salt as an example, thickener is used to solve the phase separation problem, which aims to improve the uniformity of PCMs system by using viscosity. The difference is that the use of thickener to improve the stability of hydrated salt PCMs cycle is to inhibit the loss of crystal water.

#### 2.5. Practical Application of PCMs

Different working conditions have different performance requirements for PCMs. Both organic and inorganic PCMs have their own advantages and disadvantages. Unmodified organic or inorganic PCMs cannot be directly put into practical applications.

Considering the standard operating temperature of PV cells of 25 °C, it is recommended to use PCMs with phase-change temperature range of 25–35 °C.<sup>[63]</sup> When the ambient temperature exceeds this range, the corresponding choice needs to be made according to the specific situation, resulting in the PCMs phase-change temperature used in PV–PCM systems in tropical

regions is often above 35 °C. To achieve the desired thermal management effect for PV, it is important to ensure a high latent heat of PCMs while maintaining the appropriate phase-change temperature. PCMs must meet practical application conditions such as absence of supercooling, absence of phase separation, high thermal conductivity, as well as appropriate phase-change temperature and high latent heat.<sup>[64]</sup> Table 8 summarizes the necessary characteristics of PCMs for real-world use.

### 3. PV Thermal Management Systems Integrated with PCMs

The invention of PV cells marked that PV has officially entered the stage of practical application from theoretical research.<sup>[65]</sup> PV technology has the advantages of clean and pollution free, small budget, high power, etc., which has been widely concerned.<sup>[66]</sup> However, in the actual application process, the solar radiation intensity is constantly changing. Furthermore, in addition to the process of converting light into electricity, any surplus solar energy will be transformed into thermal energy and stored in PV cells, leading to an elevation in the temperature of these cells. The rated operating temperature of PV cells is 25 °C. When the temperature of operation goes beyond 25 °C, the efficiency of converting light into electricity in PV cells will decrease, resulting in a decrease of 0.4% in output power for each 1 °C rise in temperature.<sup>[67]</sup> When the temperature of the PV cells exceeds the limit temperature, the ethylene vinyl acetate copolymer layer will liquefy, ultimately reducing the life of the PV cells.<sup>[68]</sup>

Therefore, many researchers focus on using the ability of PCMs to absorb heat during the melting process to regulate the temperature of PV cells, thereby delaying the rise of PV cell temperature. According to the study of Wongwuttanasatian et al.<sup>[69]</sup> PCM cooling may not be required when the irradiation amount is less than a certain amount (i.e., 500 W m<sup>-2</sup>). In comparison to conventional cooling techniques like water-cooling and air cooling, the utilization of PCMs in thermal management proves to be effective, cost-effective, and devoid of noise. As shown in Figure 4, the PCM thermal management unit is located on the back of the PV cell, forming a simple PV–PCM configuration.<sup>[13]</sup> To achieve the optimal effect of photovoltaic thermal management, it is appropriate to set the PCMs phase-change temperature in the range of 25–35 °C. However, in many studies, due to the influence of environmental temperature and other factors, the phase-change temperature of PCMs is often outside the aforementioned range. In this section, the relevant studies conforming to the ideal phase-change temperature range will be highlighted and cited.

To enhance electrical efficiency, there are four categories of techniques for managing the temperature of PV cells using PCMs: PV–PCM, concentrated PV (CPV)–PCM, building-integrated PV (BIPV)–PCM, and PV–thermoelectric (TE)–

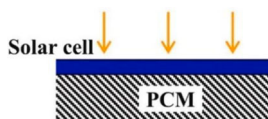


Figure 4. Simple PV–PCM configuration.

PCM. In this section, these four techniques are discussed in detail. At the end of this section, the feasibility and economics of combining PCMs and PV cells are summarized and analyzed.

### 3.1. PV-PCM

The study of PV-PCM was first documented in 2004. Huang et al.<sup>[70]</sup> conducted an application study on PCM control of PV temperature rise through experiment and numerical simulation. The finned-PV-PCM system is shown in **Figure 5**. A 2D model for heat transfer was created, where the Navier-Stokes equations and energy equations were solved. A parameterization study of the design application was also reported. Various system configurations were analyzed using experimentally verified numerical models to anticipate the temperature, velocity patterns, and formation of vortices. The PV surface temperature distribution was predicted according to different light levels and ambient

temperature. The results showed that temperature regulation can greatly improve the operating efficiency of PV. Following the previous studies, Huang et al.<sup>[71]</sup> performed an additional analysis to evaluate the effect of PCM on the heat transfer efficiency of finned-PV-PCM devices. **Figure 6** shows a PV-PCM system using aluminum fins. Setting the internal fin in the PV-PCM system can improve the temperature regulation effect of the PV cell.

When designing and researching the PV-PCM systems, the primary factor to be taken into account is the impact of weather conditions on the PV-PCM systems. The suitable phase-change temperature is the decisive factor for PCMs to play a role in PV-PCM systems. The ideal phase-change temperature of a PV-PCM system depends on the optimal operating temperature of the PV cell and the climatic conditions in different geographical regions. Furthermore, varying weather conditions also impact the TE efficiency of PV-PCM systems. Smith et al.<sup>[72]</sup> conducted a worldwide study to calculate the increase in annual energy production (AEP) of PV-PCM system. The 1D energy balance simulations utilized temporary reanalysis of climate data, including ambient temperature, irradiance, and wind speed, extracted from a global grid of  $1.5^{\circ}$  longitude by  $1.5^{\circ}$  latitude. The effect of temperature fluctuation from 0 to  $50^{\circ}\text{C}$  on the action of PCM was studied, and the ideal melting temperature of each grid position was determined. In areas with sufficient sunshine and small interannual climate change, PCMs has the best cooling effect on PV cells. With ideal PCM melting temperatures, PV generation in Mexico and East Africa is growing by more than  $6\text{ year}^{-1}$ . In Central and South America, Africa, Arabia, South Asia, and the Indonesian archipelago, the annual growth rate of PV power generation is more than 5%. Across Europe, the rise in energy production varies from a 2% increment to almost 5%. Typically, with increased average ambient temperatures, the ideal melting temperature for PCM in PV cooling also rises. Even the use of nonoptimal PCMs has the potential to greatly improve the TE performance of PV cells. Khanna et al.<sup>[73]</sup> studied the climate suitable for PV-PCM systems. The findings indicate that 1) the environment with small temperature fluctuation is more suitable for using PCMs for PV thermal regulation; 2) warm climates facilitate more efficient heat extraction in PV-PCM systems compared to cold climates; 3) the synergistic impact of PCMs and PV cells is enhanced in climates characterized by low wind speeds; 4) the PV-PCM systems show greater efficiency

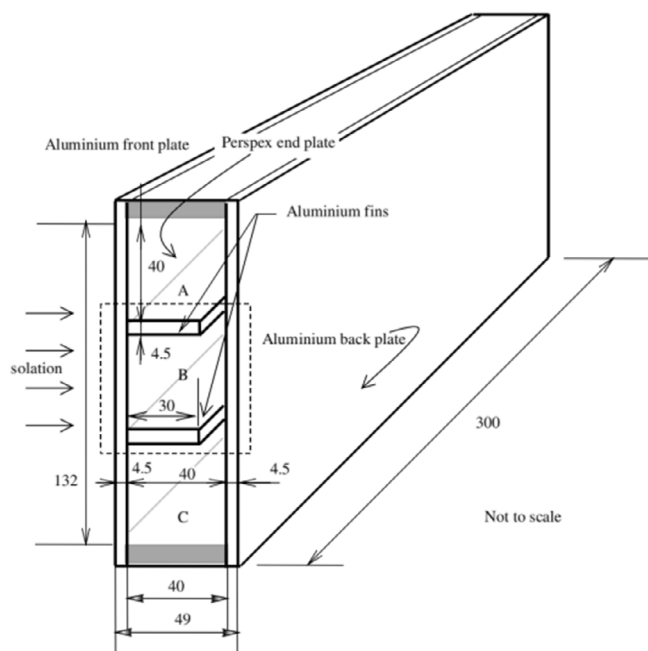


**Figure 5.** Schematic diagram of PV-PCM experimental system with inner fin (size: mm).

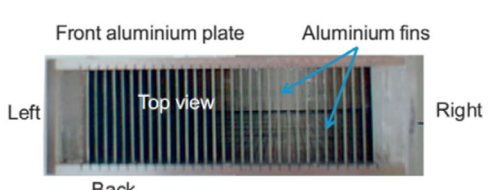


**Figure 6.** PV-PCM system with aluminum metal fins installed.

under the climate condition of strong air convection; and 5) environments with abundant solar radiation are highly favorable for PCMs to fulfill their function. Foteinidis et al.<sup>[74]</sup> collected long-term data on PV–PCM system operating under climatic conditions in the Mediterranean region, particularly Greece. According to the energy analysis, while increasing the power output of PV cells by 9.4%, the utilization of PCM cooling leads to a larger initial investment, resulting in a lower return on investment for PV–PCM systems than for PV systems. However, from an environmental point of view, the additional electricity generated by PV cooling displaces electricity dependent on fossil fuels and thus brings environmental benefits.

Once a suitable phase-change temperature has been determined, the next step is to prepare suitable composite PCMs. After the composite modification of PCM is completed, the phase-change unit is filled with PCM and placed on the back of the PV cell to prepare for the subsequent TE performance test. Rezvanpour et al.<sup>[75]</sup> studied the effectiveness of composite PCM in thermal management of PV–PCM systems through experiments and simulations. The impact of  $\text{CaCl}_2\cdot 6\text{H}_2\text{O}$  as a PCM on the regulation of PV cell temperature and enhancement of the electrical efficiency of PV cell was examined in a fully cold environment in Tehran, Iran. The experimental results were confirmed using transient system simulation program (TRNSYS) simulation software. Figure 7 displays the PV–PCM array module configuration simulated using TRNSYS. The simulation results were compared to the experimental results. According to the experimental findings, the PV–PCM system managed to decrease the PV cell's highest temperature by 26.3 °C (equivalent to a 38% reduction) in comparison to the conventional PV module. Furthermore, the PV–PCM system experienced a boost in its power generation, with an additional 1.16 W output in November and December, representing a substantial increase of 24.68%. The experimental and simulated results show a good agreement,

with a minimum difference of 0.96% and a maximum difference of 8.25%. A new composite PCM, consisting of  $\text{CaCl}_2\cdot 6\text{H}_2\text{O}$ – $\text{MgCl}_2\cdot 6\text{H}_2\text{O}$  eutectic mixture as the PCM and expanded graphite (EG) as the carrier, was prepared through physical blending by Y. Zhang and X. Zhang.<sup>[76]</sup> The experimental results showed that the latent heat of composite PCM containing 8% EG is  $171.4 \text{ kJ kg}^{-1}$ , the phase transition temperature is 27.1 °C, the supercooling degree is 0.11 °C, and the thermal conductivity is  $3.359 \text{ W m}^{-1} \text{ K}^{-1}$ . Even after undergoing 100 cycles of heating and cooling, the thermal properties of the modified composite PCM remain outstanding. By utilizing the composite PCM, the surface temperature of the PV cell can be greatly decreased, ensuring that the average temperature remains below 40 °C. PV cell can operate near their rated power for 3.5–4 h, maintaining a consistently high power output and generating 7.9% more power than PV cell alone. Karami et al.<sup>[77]</sup> prepared a paraffin–beef tallow–coconut oil (PBTCO)-based composite PCM for PV thermal regulation. EG was added to PBTCO to improve its thermal conductivity. The optimal parameters and conditions of PV/EG–PBTCO system were realized by response surface method (RSM). The results showed that adding EG to PBTCO composite PCM can greatly improve the performance of PCM, and also give PCM a strong ability to uniform the temperature distribution of PV.

Enhancing the thermal conductivity of PCMs is imperative for PV–PCM systems to enhance the TE efficiency of the system. The literature mentioned earlier primarily utilizes EG as a medium to enhance the thermal conductivity and maintain the shape stability of PCMs. In addition to EG, metal foam materials are also very effective in enhancing the thermal conductivity of PCMs as typical 3D structure additives. The permeability of metal foam has a specific impact on the transfer of heat and the capacity to store heat of PCMs. The impact of this key phenomenon on PV–PCM systems has gained significant attention.

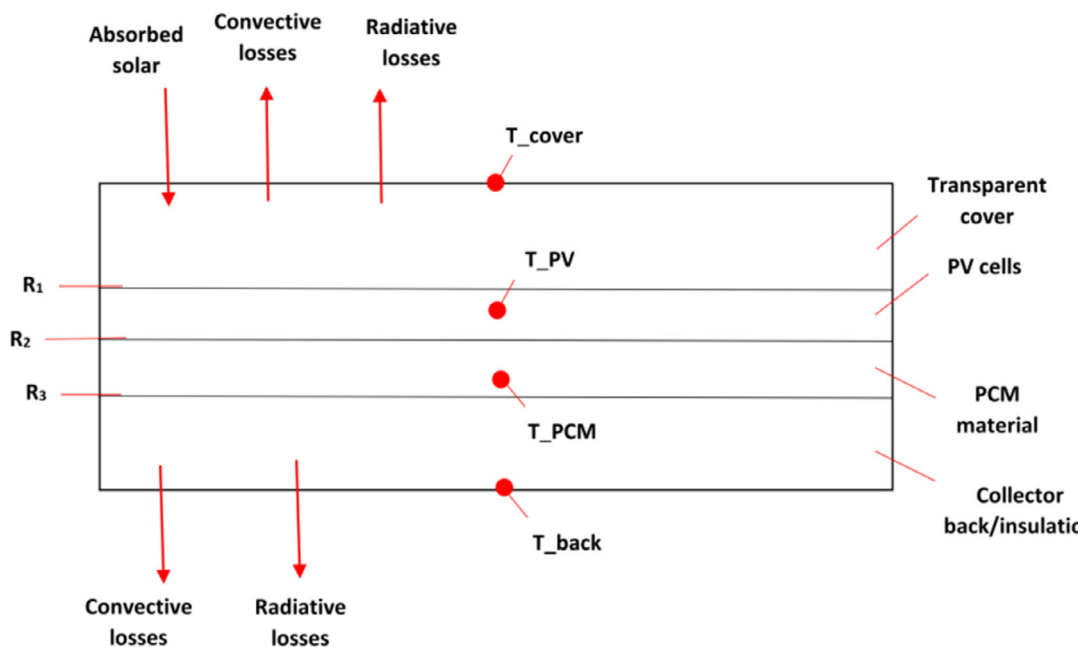


Figure 7. The PV–PCM array module configuration simulated using TRNSYS.

Li et al.<sup>[78]</sup> used the pore-scale lattice Boltzmann model to study the dynamic heat transfer characteristics of PCM after adding metal foam. During the late melting period, it was discovered that the composite PCM experienced a significant decrease in its melting rate, resulting in the formation of a prolonged solid PCM region known as the “dead zone”. To solve this problem, they proposed a unique PCM structure, which is not uniform and therefore the porosity of the dead zone is not unique. Significant improvements can be achieved in the melting rate, energy density, and power density of composite PCM by modifying the porosity of composite metal foam. In another paper, Li et al.<sup>[79]</sup> once again established the pore-scale lattice Boltzmann model, using X-ray microcomputed tomography to characterize the complex microstructure of metal foam and calculate the dynamic temperature and flow fields in common scenarios.

At present, the research of PCM in PV–PCM mainly focuses on the melting process of PCM. However, to ensure the uninterrupted use of PCMs, the solidification and heat release process of PCMs at night is also considered crucial. Nanoparticles, commonly used as 0D structure additives, have found extensive application in the study and advancement of PCMs in recent times. Nanoparticles can reduce or eliminate the supercooling degree of inorganic hydrated salt PCMs, greatly improve the thermal conductivity of PCMs, and have little effect on the latent heat loss of PCMs. Therefore, the application of nanoenhanced PCMs (NePCMs) in PV–PCM system has become a hot topic. Feng et al.<sup>[80]</sup> created a promising low subcooling nanoemulsion PCM for PV thermal management. The phase-change and thermal physical properties of OP35E paraffin nanoemulsion were studied. The results showed that the melting point of the nanoemulsion is about 34 °C, and there is almost no supercooling. During the phase change, the apparent specific heat of OP35E nanoemulsion is 2.29–3.29 times that of water, and the viscosity is slightly higher than that of water. The utilization of a nanoemulsion containing 20 wt% OP35E resulted in an additional 5.3% decrease in the temperature of the PV module compared to that of water.

After developing PCMs with excellent heat storage performance and suitable for thermal management of PV cells, researchers can turn their attention to the optimization of the heat transfer structure of PV–PCM systems. In addition to the heat transfer structure, the effect of PV cell inclination on PV–PCM system is also noteworthy.

Increasing the heat transfer area, fins improve the heat transfer between PCMs and PV cells. Fins are also the most commonly used structure to enhance heat transfer. The PV–PCM system's related research was initially conducted by Huang et al. focusing on the fin heat exchanger. However, the model they proposed in the article is a little rough, and there is a certain gap with the finned-PV–PCM system. The study of Khanna et al.<sup>[81]</sup> initiated the optimization of finned-PV–PCM system. For comparative analysis, the PV system, PV–PCM system and finned-PV–PCM system were designed, as shown in Figure 8. The findings indicated that the ideal gap between consecutive fins measures 25 cm, while the optimal thickness of the fins is 2 mm. Khanna et al.<sup>[82]</sup> published another article optimized finned PV–PCM to achieve appropriate power enhancements under different operating environments. The calculated and modeled optimal depth for installing the fin of a PV

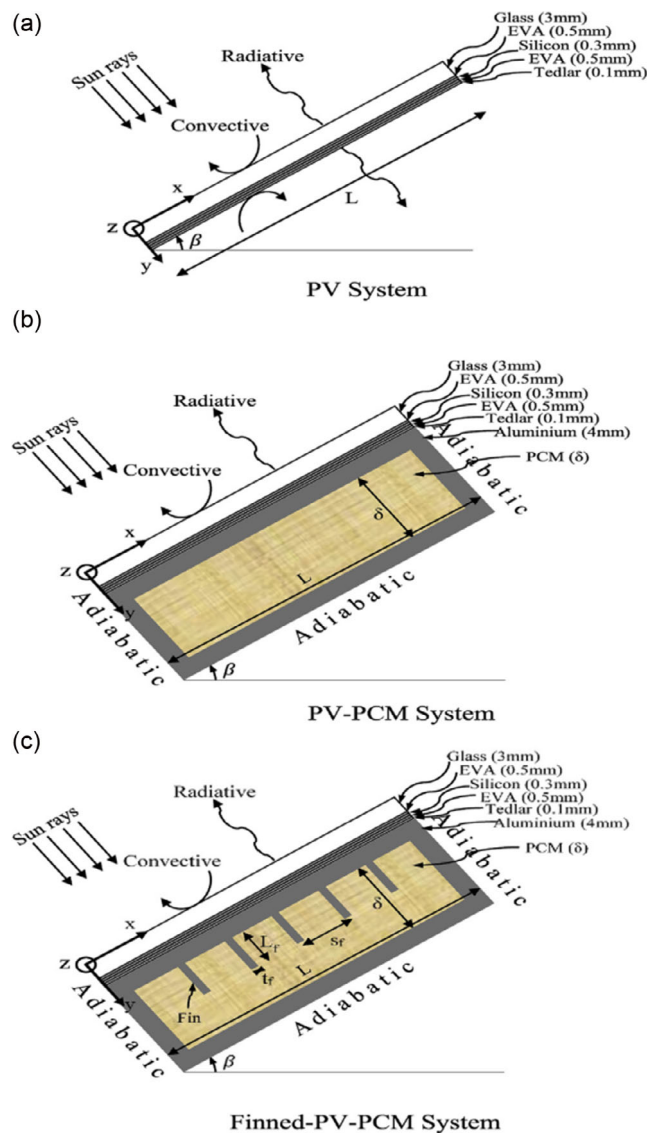


**Figure 8.** Schematic diagram of a) PV system, b) PV–PCM system, and c) finned-PV–PCM system.

cell takes into account various factors such as daily total solar radiation, wind velocity, azimuth angle, ambient temperature, melting point, distance between fins, fin depth, and fin width. Additionally, the analysis includes an examination of how different working conditions impact the installation depth. The findings indicated that with a daily total solar energy of  $5000 \text{ Wh m}^{-2}$ , the spacing between fins was adjusted to 1, 1/2, 1/3, 1/4, and 1/5 m, while the wind velocity ranged from 0.2 to  $6 \text{ m s}^{-1}$ . Consequently, the optimal depth of the PCM envelope decreased from 5.2 to 3.7, 5.6 to 4.0, 5.8 to 4.2, 5.9 to 4.3, and 5.9 to 4.3 cm, respectively. Increasing the wind azimuth from 0° to 75° led to a rise in the ideal depth of the envelope. The power generation rose from 125 to 137, 140, 142, 143, and  $143 \text{ W m}^{-2}$ , respectively. Singh et al.<sup>[83]</sup> studied the structure of the finned-PV–PCM system and developed a mathematical model. The investigation examines the arrangement of the fin PV–PCM

system considering various factors such as wind direction, wind speed, ambient temperature, phase-change temperature, and limited dimensions. The results showed that the power enhancement duration of PV–PCM system increased from 6.1 to 7.3 h when the wind azimuth changes from  $75^\circ$  to  $0^\circ$  under the constraint of 5 cm fin depth. Moreover, the wind speed decreased from 6 to  $1 \text{ m s}^{-1}$  resulting in a decrease in the duration of the power enhancement from 7.8 to 6.1 h.

Over the past few years, scientists have also investigated other heat transfer structures in addition to fins and applied them to PV–PCM systems. Akshayveer et al.<sup>[84]</sup> studied a design method for a new PV cell with an overhead PCM housing, as shown in Figure 9. After studying different design schemes and analyzing the characteristics of the melt front, a final design scheme that was deemed optimal was proposed. The new layout enhances the absorption of solar radiation by approximately 17-fold compared

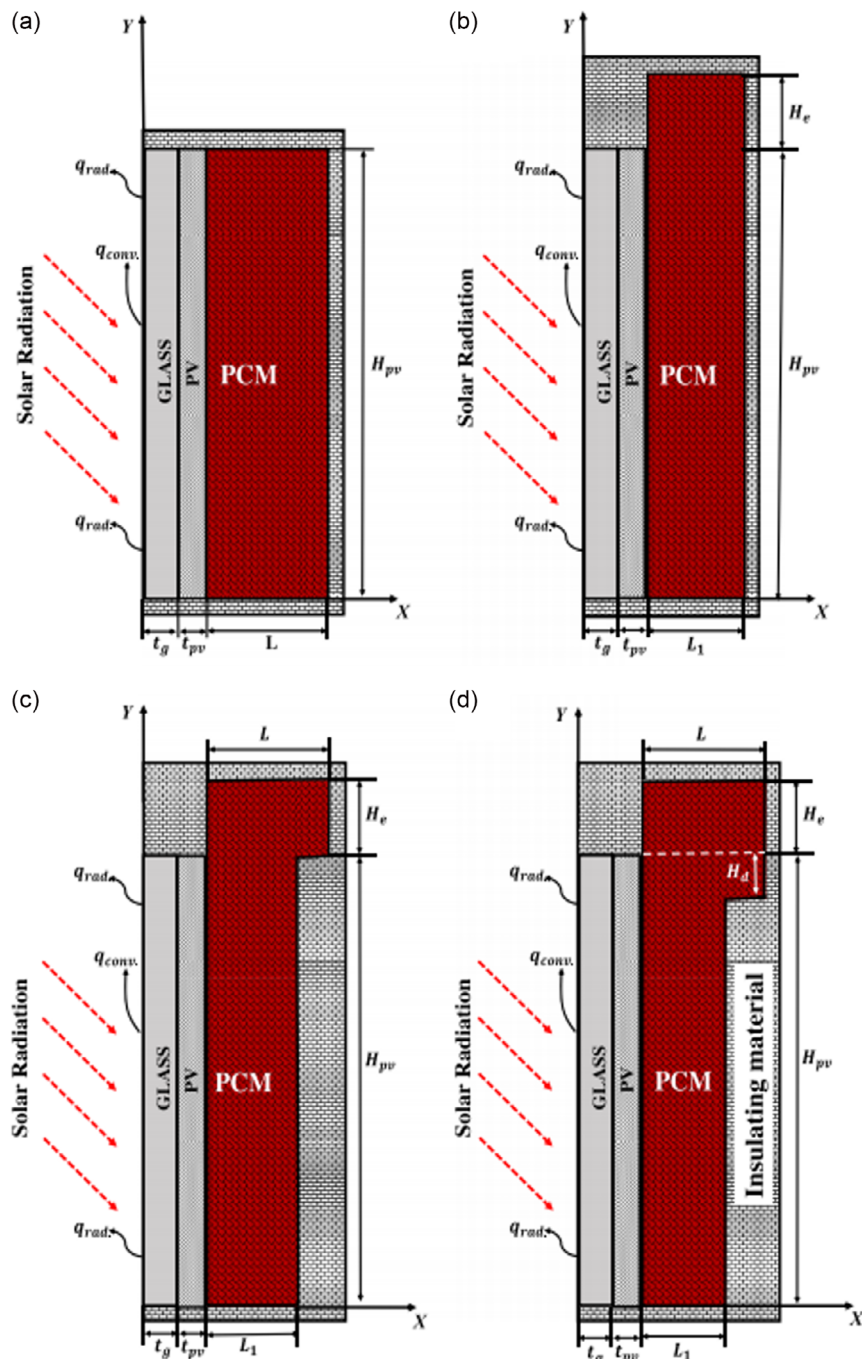


**Figure 9.** The 2D view of PV cell with integrated PCM enclosure: a) rectangular enclosure, b) rectangular enclosure with extension  $H_e$ , c) rectangular enclosure with overhead tank extension  $H_e$ , and d) rectangular enclosure with modified overhead tank extension  $H_e$  and depression  $H_d$ .

to traditional PV systems. This leads to an augmented utilization rate of solar radiation and an approximately 10% increase in energy storage density. By strategically distributing PCM, the duration of the quasi-steady region primarily influenced by convection is extended, indicating that the melting rate of PCM surpasses that of the conventional rectangular design. Research has indicated that the PV cell's electrical conversion efficiency can reach approximately 12%. Khanna et al.<sup>[85]</sup> proposed thermal conductivity enhancing containers (TCEC) that enables the PCM to extract heat from all directions rather than just the front, thereby improving the thermal conductivity of the PCM container. The electrical efficiency of the PV cell was thus improved. **Figure 10** shows the experimental setup of the PV-TCEC-PCM system. PCM was inserted into the TCEC and connected to the rear of the PV cell. An analysis was conducted on the enhancement of the melting process, heat retention rate, efficiency of charging, and performance of PCM in PV. TCEC can increase the average melting efficiency of PCM from 49% to 62%. Furthermore, employing TCEC-PCM has the potential to enhance the mean heat storage rate from 249 to 302 W m<sup>-2</sup>, as well as elevate the PV electrical efficiency from 17.6% to 19.2%. Decreasing the PCM container's inclination from 45° to 0° resulted in a 32% decrease in melting efficiency. Shoail et al.<sup>[86]</sup> designed a new type of heat sink for use on the back of PV cells. The suggested radiator comprises a collection of perforated cylindrical bars. The proposed thermal management model was studied by experiments and simulations. The TE performance of PV cell before and after radiator improvement is compared. Conduction and heat transfer are utilized by the heat sink to absorb the heat from the PV cell's rear surface, thereby enhancing the heat transfer area. During the test, the temperature of the PV cell dropped by 5.18 °C, and the output voltage increased by 0.53 V. Compared to the PV-PCM system before the radiator improvement, the PCM efficiency is improved by 2.9%. Using the validated numerical model, the impact of wind velocity and angle of incidence on the enhanced PV module integrated with PCM was investigated. The findings indicated that the combined PCM effectively enhances the PV module's power output.

In practical engineering, PV cells are usually tilted according to the local latitude, rather than placed vertically. Studying the impact of tilt angle on the TE characteristics of PV cells and

the thermal properties of PCMs in PV-PCM systems holds immense importance. Khanna et al.<sup>[87]</sup> tested the performance of a tilted PV-PCM system. The effects of tilt angle, wind direction, wind speed, ambient temperature, PCM melting point temperature on PCM heat absorption rate, PCM melting process, and PV cell temperature were studied. Increasing the tilt angle from 0° to 90° resulted in a decrease in PV cell temperature from 43.4 to 34.5 °C, leading to a rise in PV cell efficiency from 18.1% to 19%, as indicated by the findings. Comparing the PV-PCM system to a solitary PV cell revealed that incorporating PCM resulted in a 19°C reduction in the operating temperature of the PV cell, while simultaneously boosting the efficiency from 17.1% to 19%. Variji et al.<sup>[88]</sup> investigated the effect of tilt angles on the enhancement of natural convection through liquid PCM, including different angles from 0° to 90°. The findings indicated that enhancing the inclination angle promotes the occurrence of natural convection and facilitates the heat transfer of molten PCM **Figure 11**.

In addition to the previous research areas, there are other areas of research on PV-PCM systems, such as the electrical efficiency of PV-PCM systems under different operating conditions, and exploring how PCMs can extend the PV electrical enhancement period. These aspects deserve equal attention. Nouira et al.<sup>[89]</sup> studied the performance of PV-PCM system under different dust densities. The electrical power is reduced by approximately 1.2, 2.8, and 3 W, respectively, due to dust densities of 3, 6, and 9 g m<sup>-2</sup>. Khanna et al.<sup>[90]</sup> studied the extension of the duration of PV electrical enhancement, the increase of power and the improvement of electrical efficiency caused by the addition of PCM under different operating conditions. According to the findings, as the wind angle reduces from 75° to 0°, the duration of electric enhancement in the 5 cm deep PCM box increases from 7.0 to 8.6 h, while the power increase decreases from 17.6 to 13.6 W m<sup>-2</sup>. The electrical enhancement period decreased from 12.6 to 7.1 h when the ambient temperature increased from 289 to 299 K. Adibpour et al.<sup>[91]</sup> used PCM cooling to improve the power output of the tracking PV cell, as shown in **Figure 12**. The experiment was conducted outdoors in Melbourne, Australia. The results showed that the efficiency of PV-PCM system is 4.6% higher than that of PV on average, and the maximum efficiency increase can reach 6.8%.

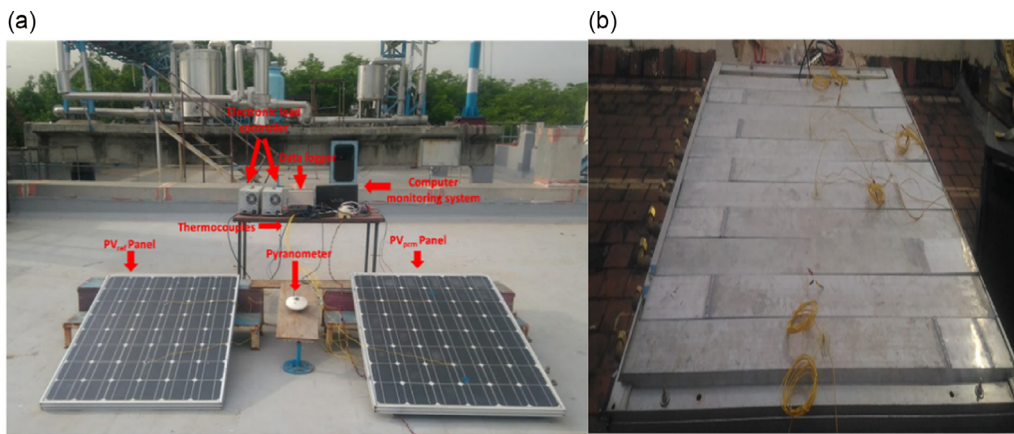


**Figure 10.** a) Reference PV system and PV-TCEC-PCM system; b) back of PV-TCEC-PCM system.

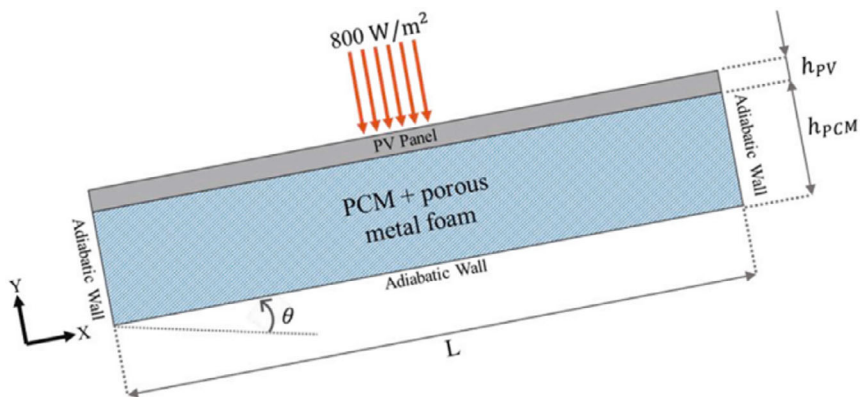


**Figure 11.** Schematic diagram of PV–PCM system used to study the influence of tilt angle on natural convection.

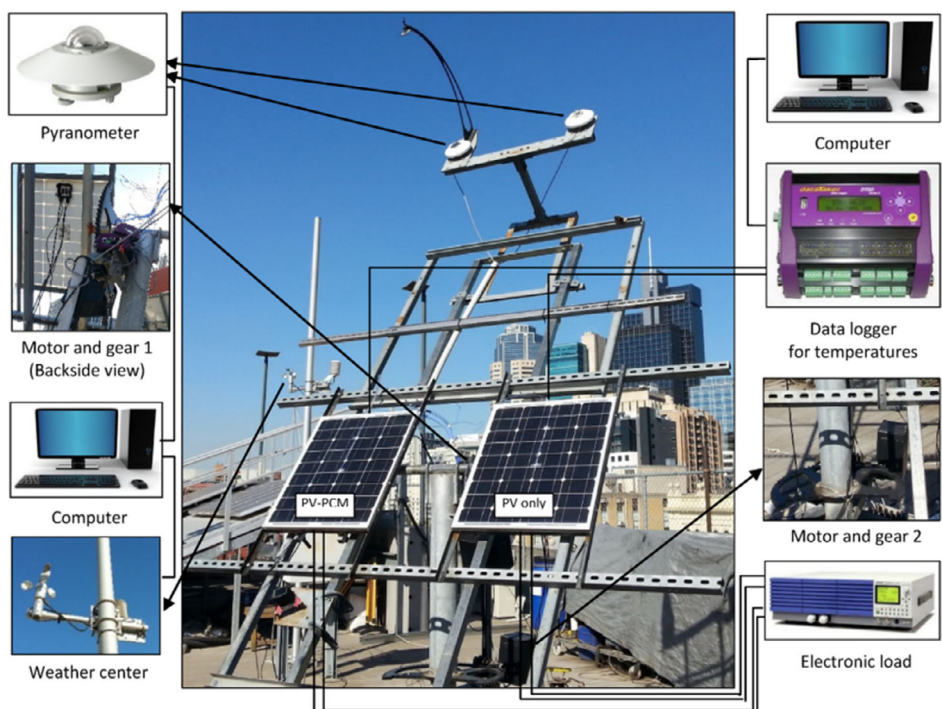


**Figure 12.** PCM-tracking PV cell experimental setup.

In summary, the related research of PV–PCM mainly involves the development of high-performance PCM, PCM container (with extended surface, i.e., fin type, etc.), and the influence of inclination angle on the melting characteristics of PV modules. At present, the means to improve the thermal conductivity of PCMs is focused on the PCMs itself, that is, the use of thermal conductivity enhancer to improve the thermal conductivity of PCMs. The degree of adhesion between PCMs and heat transfer structure determines the contact thermal resistance. The use of flexible PCMs can increase the degree of adhesion between PCMs and heat transfer structure to reduce the contact thermal resistance. At present, the optimization of heat transfer structure of PV–PCM systems is mostly experimental, and few studies have been advanced to the theoretical level. In the future, more

theoretical research ideas and methods such as genetic algorithm (GA), back propagation (BP) neural network, and big data can be applied to obtain the optimal shape, size, and quantity of heat transfer structures.

### 3.2. CPV–PCM

Sunlight will be refracted after being projected on the PV cell, which is unavoidable. Sunlight that is reflected to the outside environment can be returned to the PV cell using a lens or a flat mirror to make the best use of sunlight, a technology known as CPV. CPV improves the efficiency of solar energy with little overhead. Theoretically, CPV has the potential to generate approximately double the electrical advantage of PV.<sup>[92]</sup>

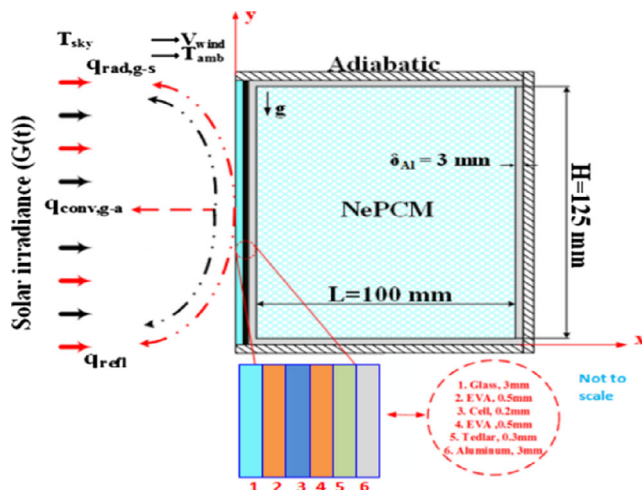


**Figure 13.** Schematic diagram of a rectangular CPV–NePCM system with PV cell layer.

But at the same time, CPV also causes the operating temperature of the PV cells to increase, so more accurate and effective thermal control of CPV technology is needed. For CPV–PCM systems, PCMs are not only required to have higher phase-change

temperature, thermal conductivity, and latent heat, but also to achieve the optimal heat transfer structure design between PCMs and PV cells.

Because CPV–PCM has more stringent performance requirements for PCMs, NePCMs has greater potential and play space in CPV. Zarma et al.<sup>[93]</sup> tested the performance of the CPV–NePCM hybrid system when the solar concentrating ratio (CR) was 20, as shown in **Figure 13**. The overall performance of the CPV system was examined by studying the impact of various nanoparticles ( $\text{Al}_2\text{O}_3$ ,  $\text{CuO}$ , and  $\text{SiO}_2$ ) at addition ratios of 1 and 5 wt%. A 2D hybrid model composed of PV and NePCM radiators was established and numerically simulated. The findings indicated that the inclusion of  $\text{Al}_2\text{O}_3$  greatly enhances the thermal conductivity of PCM, leading to improved heat transfer, accelerated melting rate, and decreased temperature of the PV cell when compared to  $\text{CuO}$  and  $\text{SiO}_2$  nanoparticles. Sivashankar et al.<sup>[94]</sup> simulated and studied the temperature of CPV in the CPV–NEPCM system, as shown in **Figure 14**. Commercially available OM35 paraffin was used as PCM and graphene nano-platelets (GNP) as carrier. The heat sink is linked to the heater, allowing the PCM to absorb and store the heat generated by the heater. The study focused on the electrical efficiency of CPV using NePCM and its comparison with CPV using pure PCM. The findings of this research demonstrated that NePCM has a

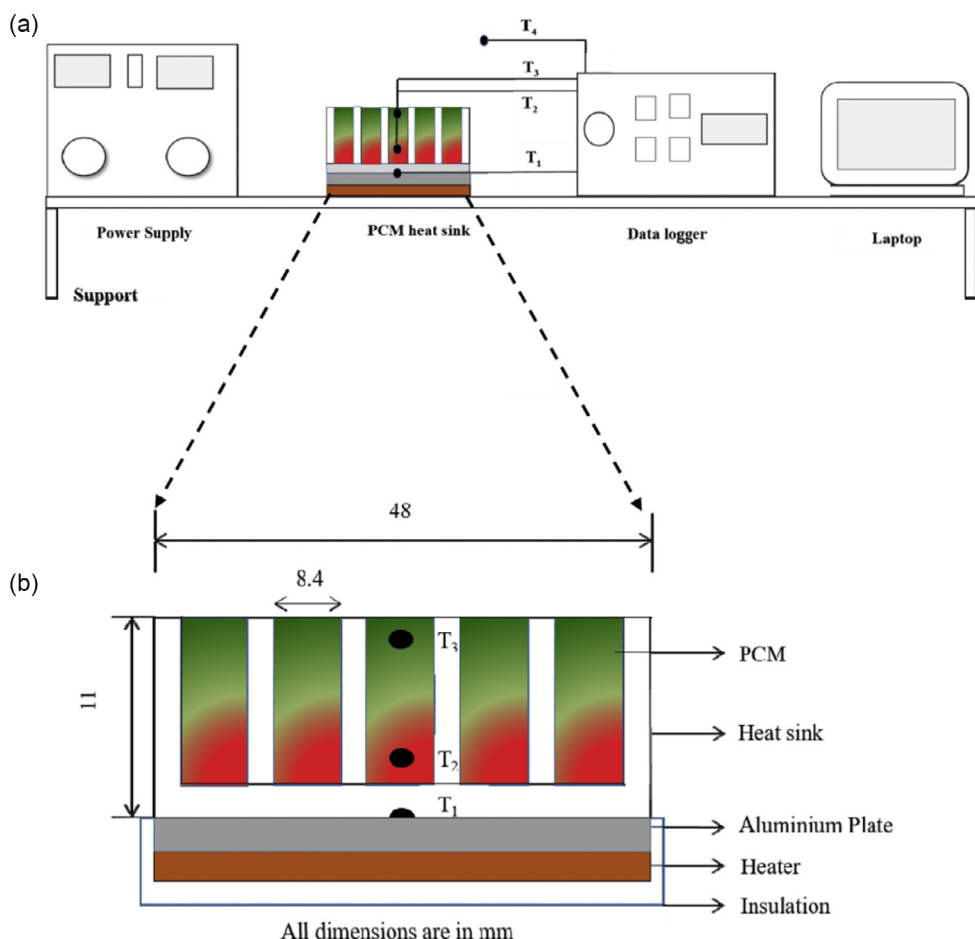


**Figure 14.** a) Diagrammatic representation of experimental test equipment for CPV–NePCM; b) NePCM heat sink.

notable impact on lowering the temperature of CPV cells, consequently enhancing the power output and efficiency of CPV cells. With the addition of 0.5 vol% NePCM, CPV experienced a 7% boost in output power and a 6% improvement in efficiency.

Optimization of the heat transfer structure of CPV–PCM systems is another focus. Emam and Ahmed<sup>[95]</sup> built a new CPV–PCM system. As shown in **Figure 15**, the system consists of four different types of PCM heat sinks: single cavity, triple parallel cavity, five parallel cavity, and triple series cavity structures. To forecast the fluctuating temperature variations at various CRs (10 and 20), a model incorporating a heat sink of PCMs was developed for a 2D integrated PV layer. The model was simulated and verified by the existing experimental data. Compared to single cavity and triple series cavity radiator configurations, the temperature of the PV cell was significantly reduced by the parallel cavity radiator configurations of triple and five. Moreover, employing five parallel cavity heat sinks can significantly enhance the evenness of temperature in PV cells. The various configurations of PCMs with a triple series cavity structure also showed a notable improvement in temperature consistency. Manikandan et al.<sup>[96]</sup> studied a CPV–PCM system with built-in heat sink using COMSOL software. To maintain the consistency of the CPV module and meet the temperature requirements of the work, the PCM is integrated in the rear of the CPV. The change in CPV performance was achieved by changing the PCM filling amount and solar CR. The findings indicated that incorporating PCM into CPV module leads to a significant decrease in temperature compared to CPV module without PCM. The recorded CPV temperature reached 55 °C, while the height of the PCM measured 0.75 mm. The temperature of the CPV in the radiator was brought down to 32 °C, while the height of the PCM measured 3 mm. Throughout the PCM melting process, the CPV temperature remained consistent between the 25th and 120th second. Solar CR maintained constant value 3. The findings indicated that the CPV module's output power and efficiency rise as the PCM filling in the radiator

increases. In normal operating circumstances, when the solar CR is 3 and the PCM height is 3 mm, the CPV with PCM exhibits a 27% increase in output power and a 22% increase in efficiency compared to a CPV without PCM. Elsabahy et al.<sup>[97]</sup> proposed a new encapsulated PCM design, combining it with the CPV system to improve the photoelectric conversion efficiency and thermal efficiency of the CPV system. The optimized layout improves the thermal conductivity of the heat sink and is conducive to the rapid loss of CPV heat. Two distinct groups of PCM enclosures were evaluated and contrasted with a traditional radiator that lacked a casing. To assess the performance of the system, a 2D CPV model was created for the integrated package PCM heat sink. Numerical simulation was conducted on the model and its accuracy was confirmed through experimental and numerical data. The results showed that the average temperature of the specially packaged PV cell is reduced by 16 °C and the temperature nonuniformity is reduced by 24 °C compared with the traditional radiator. Special packages can help increase power output, store thermal energy, and reduce heat loss. The system experienced a 21.3% increase in its overall electrical efficiency and a 5.29% increase in its thermal efficiency.

### 3.3. BIPV–PCM

The construction sector accounts for about 40% of global CO<sub>2</sub> emissions.<sup>[98]</sup> Hence, implementing strategies to decrease the energy usage of structures or supplying them with sustainable energy sources will immensely contribute to the advancement of sustainability. The application of PV modules in buildings is a major way to achieve this goal, and BIPV is referred to as BIPV for short. BIPV's effectiveness relies on factors such as the amount of sunlight received, surrounding temperature, and the building's position and alignment.<sup>[99]</sup> BIPV–PCM systems use PCMs to achieve temperature regulation of PV cells and optimize the performance of BIPV systems. The study of BIPV–PCM systems not only involves the development of PCMs and heat transfer analysis of PCMs and PV cells, but also emphasizes the importance of integrating PCMs to improve the comfort and energy efficiency of PV buildings.

Kant et al.<sup>[100]</sup> studied the effect of different nanoparticles on the operating temperature of BIPV. The analysis of computational fluid dynamics took into account the transfer of heat and mass in the NePCM system located behind the BIPV. Four different concentrations of nanoparticles were mixed with n-octadecane PCM. To enhance the thermal conductivity of PCM, nanoparticles such as nano-Al<sub>2</sub>O<sub>3</sub>, nano-Cu, nano-CuO, and nano-TiO<sub>2</sub> have been employed. By adding an appropriate quantity of nanoparticles, the findings indicated a substantial reduction in the operational temperature of BIPV. The cooling effect of nano-Cu is the best, and the cooling effect of nano-TiO<sub>2</sub> is the worst. By maintaining a concentration of 5% of nano-Cu particles, it is possible to keep the panel temperature below 40 °C for approximately 60 min. With a concentration of 5% nano-Cu, it took a maximum of 56 min for the PCM to fully melt. In Rae–Bareilly's laboratory (26.2345°N, 81.2409°E), a 3 day simulation test revealed that incorporating nano-Cu particles into PCM can effectively lower the operational temperature of PV cells in actual weather conditions. The maximum operating

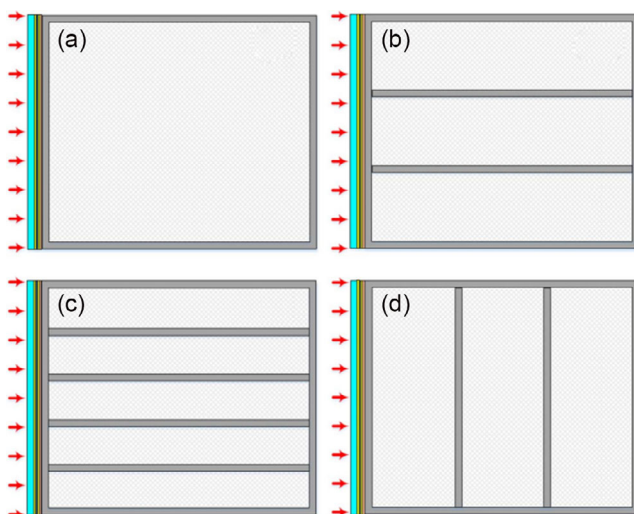


**Figure 15.** Four types of PCM heat sink configurations were tested: a) single cavity, b) triple parallel cavity, c) five parallel cavity, and d) triple series cavity.

temperature difference on the first, second, and third days was 1.65, 1.19, and 1.15 °C, respectively, at around 12:50 PM. Karthick et al.<sup>[101]</sup> prepared binary eutectic PCM by melt blending method using  $\text{Na}_2\text{SO}_4 \cdot 10\text{H}_2\text{O}$  and  $\text{Zn}(\text{NO}_3)_2 \cdot 6\text{H}_2\text{O}$ . DSC results showed that 70 wt%  $\text{Na}_2\text{SO}_4 \cdot 10\text{H}_2\text{O}$  + 30 wt%  $\text{Zn}(\text{NO}_3)_2 \cdot 6\text{H}_2\text{O}$  was the best eutectic PCM for BIPV. The prepared eutectic mixture will be used in a building-integrated semitransparent PV PCM (BISTPV-PCM) device to control the temperature of the BISTPV panel, thus comparing it to a BISTPV panel without PCM, as shown in Figure 16. The experiment was conducted in 2018 under outdoor environmental conditions in Kovilpati district, Tamil Nadu, India. Compared to the PCM-less system, the BISTPV-PCM system experienced a decrease in its peak temperature, reaching only 12 °C. By utilizing PCM, the BISTPV module's annual power output rose from 34 287 W to 37 024 W h year<sup>-1</sup>.

Karthick et al.<sup>[102]</sup> compared the performance of BIPV and BIPV-PCM systems. Figure 17 displays the schematic diagram of the BIPV-PCM module. They conducted an outdoor evaluation of both systems installed on the facades of laboratories in Kovilpati district, Tamil Nadu, India. For thermal regulation, the BIPV-PCM system utilized  $\text{Na}_2\text{SO}_4 \cdot 10\text{H}_2\text{O}$  as the PCM. The focus of the research is to improve the TE properties of BIPV by adding PCM. An analysis was conducted on different factors including power production, solar heat gain, temperature of the module surface, and electrical efficiency. By observing, it has been discovered that the BIPV-PCM system sustains a reduced maximum temperature compared to the reference BIPV, thereby enhancing the efficiency of the BIPV-PCM battery conversion. The experimental findings indicated that the BIPV-PCM system exhibits a 10% enhancement in electrical efficiency when compared to the reference BIPV module, alongside an 8 °C reduction in surface temperature. Sun et al.<sup>[103]</sup> inserted PCM into the walls of buildings to reduce the energy consumption of air conditioning and the resulting carbon emissions. They conducted simulations to analyze the thermal and electrical characteristics of BIPV-PCM buildings using four distinct volume fractions of PCMs, and then compared these findings to those of a BIPV building. To validate the simulation findings, a BIPV-PCM system building experimental apparatus was created and constructed, as depicted in Figure 18. According to the findings, the system's peak demand load in summer is decreased by 47% when incorporating 5.2 vol% PCM, and the peak value is shifted by 1 h. Three distinct optimization objectives were

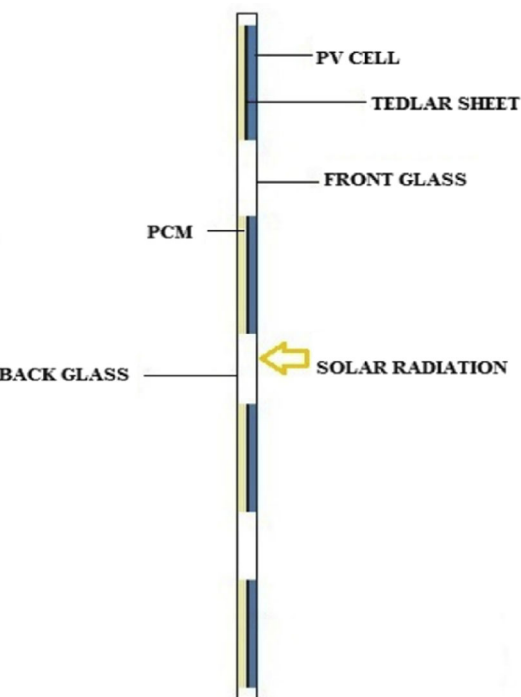


Figure 17. Schematic diagram of BIPV-PCM system.

pursued during the optimization process: achieving the highest level of building self-balance, maximizing PV self-consumption, and minimizing the interaction between the building and the grid. Buildings utilizing PCM experience increased economic benefits as a result of decreased peak demand load. The utilization of 5.2 vol% PCM in a building with an area of 6.25 m<sup>2</sup> resulted in a decrease of 11.58 kg in carbon emissions when compared to the standard building. Jo et al.<sup>[104]</sup> designed five scenarios to study the BIPV-PCM system. With the exception of scenario 1, all scenarios assumed PV equipment installed on the roof surface. PCM was used on the back of the PV cell in scenario 3, while scenario 4 involved the addition of a brick layer infused with PCM to the roof surface. In scenario 5, the techniques of scenario 3 and scenario 4 were combined and applied. By installing PV cells to generate electricity, energy saving was achieved, and the overall load reduction rate was up to 22.55%. The minimum payback period (PPB) calculated is 7 years, which is reasonable. Option 4 was considered the best retrofit plan based on cost and energy. To sum up, building retrofits using PCMs can lead to significant cost and energy savings.

### 3.4. PV-TE-PCM

The utilization of a TE generator as an efficient active cooling mechanism for PV cells enhances the power generation of the system by harnessing the electricity generated from the temperature disparity. This feature makes PV-TE a promising application. The power generation efficiency of PV-TE systems can be enhanced by incorporating PCMs, as discovered by certain researchers. Metwally et al.<sup>[105]</sup> used TE generator and PCM for PV cell heat dissipation. The heat sources of TE generator

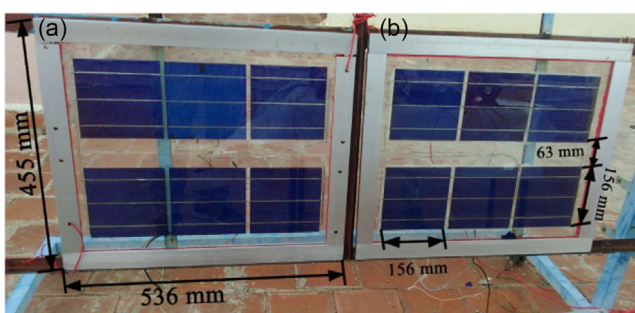
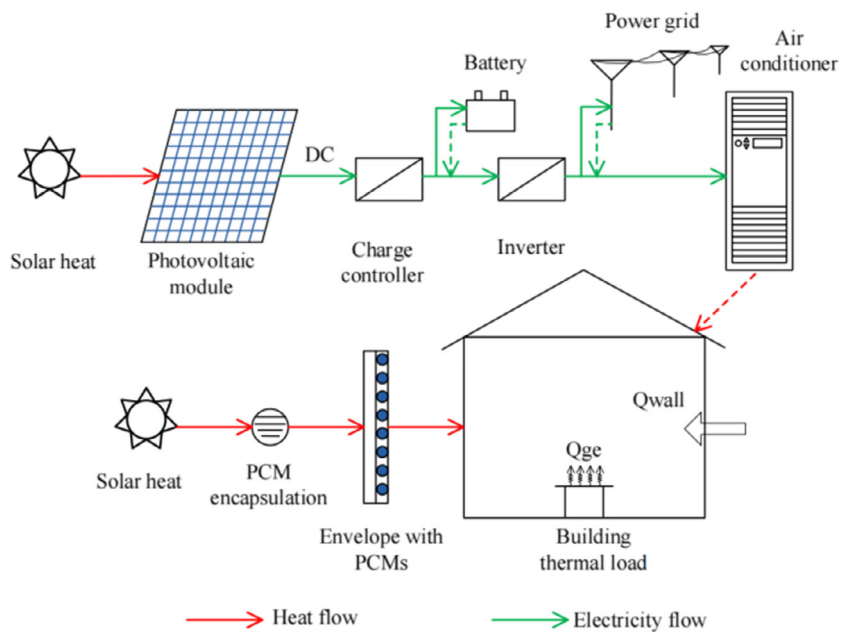


Figure 16. a) BISTPV-PCM system; b) BISTPV without PCM system installed.



**Figure 18.** A schematic of a building with PCMs and PV systems.

are PV temperature and PCM temperature. By utilizing the hybrid cooling technique, the PV cell remained at a consistent temperature for a duration of 4 h, experiencing a temperature decrease from 332 to 295 K, resulting in a remarkable reduction of approximately 60%. In favorable atmospheric conditions, the PV cell's efficiency experienced a 3.5% enhancement, leading to a 30% surge in power generation. The PV cell's enhanced efficiency can remain stable for 10 h, even when exposed to varying levels of radiation. Yusuf and Ballikaya<sup>[106]</sup> performed an

extensive numerical investigation on CPV, CPV-PCM, CPV-TE, CPV-PCM-TE, and CPV-TE-PCM systems within the COMSOL multiphysical environment. **Figure 19** and **20** show the model built. The findings indicated that the CPV-PCM, CPV-TE, CPV-PCM-TE, and CPV-TE-PCM achieved energy conversion efficiencies that were 34.8%, 97.3%, 106.5%, and 114% greater than the energy conversion efficiency of the individual CPV system, respectively. The findings also indicated that the CPV-TE-PCM configuration outperforms alternative

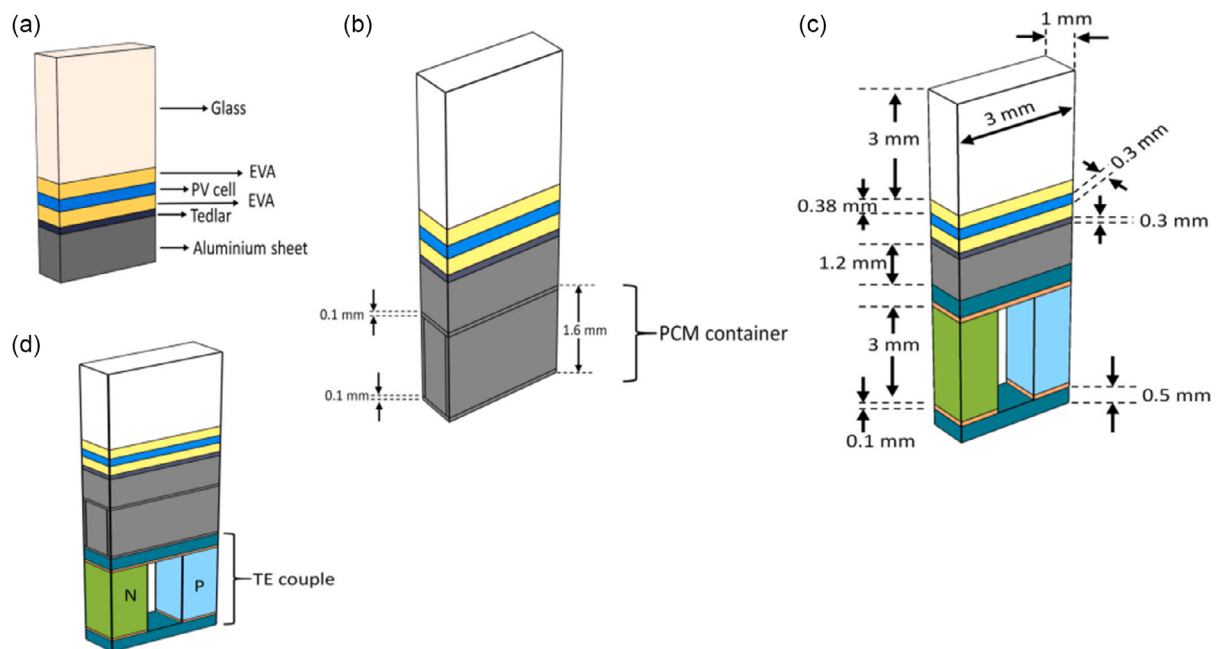


**Figure 19.** Proposed models: a) independent CPV, b) CPV-PCM, c) CPV-TE, and d) CPV-PCM-TE.

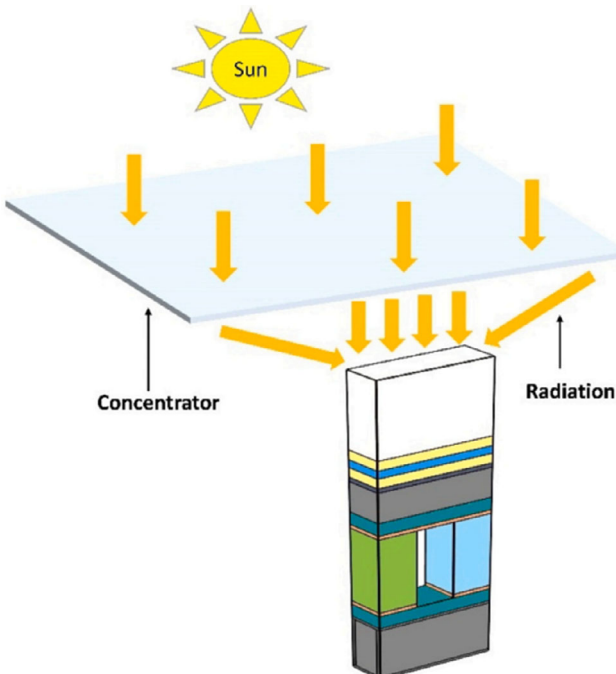


Figure 20. Model for CPV-TE-PCM.

structures as it generates a significant temperature gradient, thereby improving the efficiency of the TE generator.

### 3.5. Feasibility and Economy of PV Cells and PCMs Coupling

Studies on PV systems with integrated PCM are summarized in Table 9.

The previous studies are all experimental or simulation studies carried out in a certain period of time. In practical use, it is insufficient to solely rely on conducting experiments and analysis for a few days or a single season to evaluate the performance of the PV-PCM system. The efficiency of the PV-PCM system is somewhat influenced by the ability to consistently generate power throughout the entire year.

Zhao et al.<sup>[107]</sup> used the enhanced conductivity method to simulate the convective effect and built a 1D thermal resistance model. The model was then validated using experimental data, successfully achieving a favorable trade-off between precision and simplicity. The utilization of this model enables the evaluation and enhancement of the efficiency of PV-PCM systems on a seasonal and yearly basis. Figure 21 illustrates the PV-PCM system's experimental design. The findings indicated that the system exhibits varying behavior in accordance with distinct weather conditions. PV-PCM systems that utilize PCMs with high phase-change temperatures typically exhibit good performance during the summer months, but during the winter, heat transfer may be hindered due to the PCMs' inability to melt in cold temperatures. The maximum yearly production increased by 2.46% in comparison to the PV system used as a reference. This value is not as high as that recorded in most short-term studies conducted under sunlight conditions or in controlled

environments. In addition, there is a lack of an economic analysis section for substantial improvements in PCMs efficiency or for the development of cogeneration. This may hinder the practical implementation of PV-PCM systems at this point.

In low-temperature areas, the presence of PCMs in winter not only does not promote thermal management, but also acts as a thermal resistance, hindering the heat transfer of PV-PCM systems. In subsequent studies, it will be important not only to enhance thermal properties in PCMs, including heat conduction and latent heat, and more efficient heat transfer structures, but also to address the problems caused by PCMs units in winter. Currently, the issues of PV-PCM system during winter can be addressed through the following approaches: 1) implementing multi-tiered PCMs with varying phase-change temperatures, which are determined based on the climate attributes of different seasons; 2) establishing an active temperature control system to aid in thermal management when PCMs are ineffective; 3) designing more appropriate latent heat storage devices for regions experiencing prolonged periods of low or subzero temperatures in winter, enabling their removal from the PV cells during such weather conditions.

From an economic perspective, the utilization of heat energy collected by PCMs in the PV-PCM system can significantly reduce the PBP of the system. In short, the limitations of passive cooling in practical applications can be reflected in terms of practicality and economy. Despite the higher initial cost and increased energy consumption, the incorporation of liquid cooling into PV-PCM systems can continuously transfer and utilize heat energy through liquid circulation, thereby improving the energy efficiency of PV cells.<sup>[108]</sup> With the introduction of active cooling technology such as water-cooling into PV-PCM system, PV/T-PCM system came into being.

## 4. PV/T Systems Integrated with PCMs

The PV/T-PCM systems can be categorized based on the cooling medium into three types: air-cooled, water-cooled, and nanofluid PV/T-PCM systems.

### 4.1. Air-Cooled PV/T-PCM Systems

At normal temperature, Table 9 displays the thermal conductivity of air, water, and ethylene glycol. The table clearly demonstrates that air has significantly inferior heat transfer performance compared to water and ethylene glycol. Consequently, the effectiveness of air cooling is evidently inferior to that of liquid cooling. In addition, the heat energy collected by air is difficult to utilize compared to the use of liquid working media such as water. The aforementioned unfavorable factors greatly restrict the actual implementation of air-cooled PV/T-PCM system, so there are few related studies on air-cooled PV/T-PCM system. This does not imply that such studies are insignificant. Their research methods and ideas have certain reference value for the research of water-cooled PV/T-PCM system Table 10.

Choubineh et al.<sup>[109]</sup> discussed the influence of PCM configuration on the efficiency of air-cooled PV system through experimental research. By utilizing a 6 mm thick PCM plate, the findings from the experiment indicated a decrease in the mean

**Table 9.** Research on PV system with integrated PCM.

System types	PCMs	Highlights	Reference
PV-PCM	Paraffin	<p>A 2D model for heat transfer was created, where the Navier–Stokes equations and energy equations were solved.</p> <p>A parameterization study of the design application was also reported.</p> <p>Various system configurations were analyzed using experimentally verified numerical models to anticipate the temperature, velocity patterns, and formation of vortices.</p> <p>The PV surface temperature distribution was predicted according to different light levels and ambient temperature.</p>	[70]
PV-PCM	Paraffin	<p>PCM can be used to passively limit the temperature rise on PV.</p> <p>Effectiveness is limited by low thermal conductivities and crystallization segregation.</p> <p>Experimental evaluation of the effects of convection and crystalline segregation.</p> <p>Internal fins improve the temperature control of the PV in a PV–PCM system.</p>	[71]
PV-PCM	Paraffin	<p>PCMs can passively cool PV cells to increase energy output.</p> <p>A global numerical analysis of PV energy output with PCM cooling was presented.</p> <p>The most promising locations for PCM cooling are in the tropics.</p> <p>A relative performance improvement of over 6% is possible in some regions.</p> <p>A suboptimal PCM melting temperature still produces a beneficial energy output enhancement.</p>	[72]
PV-PCM	Paraffin	<p>Climates with less variations in ambient temperature are more suitable for PV–PCM.</p> <p>Cold climates are less suitable for heat extraction by PCM from PV.</p> <p>PCM integration with PV performs better in climates having low wind speed.</p> <p>PV cooling using PCM is more effective for climate with wind flow across the system.</p> <p>Climates having high solar radiation are better for PCM systems.</p>	[73]
PV-PCM	Paraffin	<p>The environmental performance of a PV–PCM was examined in Mediterranean.</p> <p>PCM increases the total environmental footprint by ≈22% compared to a standalone PV.</p> <p>Cooling from PCM increases electricity output also increases by 9.4%.</p> <p>Displaced electricity from the grid leads to large environmental gains.</p> <p>Results were sensitive to changes in PV's electrical efficiency and useful life.</p>	[74]
PV-PCM	CaCl <sub>2</sub> ·6H <sub>2</sub> O	<p>CaCl<sub>2</sub>·6H<sub>2</sub>O as a PCM was used to improve the PV module performance in Tehran, Iran.</p> <p>PCM reduced the PV surface temperature by 38% maximally in a cold environment.</p> <p>Power output of PV–PCM cell was increased averagely by almost 24.7%.</p> <p>The highest TRNSYS modeling error in temperature drops was 8.25%.</p> <p>The maximum TRNSYS simulation error in power output was 1.59%.</p>	[75]
PV-PCM	CaCl <sub>2</sub> ·6H <sub>2</sub> O–MgCl <sub>2</sub> ·6H <sub>2</sub> O	<p>CaCl<sub>2</sub>·6H<sub>2</sub>O–MgCl<sub>2</sub>·6H<sub>2</sub>O as PCM, SrCO<sub>3</sub> as nucleating agent, HEC as thickening agent, and EG as adsorption matrix were successfully prepared.</p> <p>The phase-change temperature was 27.1 °C, the degree of supercooling was 0.11 °C, the latent heat of phase change was 171.4 kJ kg<sup>-1</sup>, and the thermal conductivity was 3.359 W m<sup>-1</sup> K<sup>-1</sup>.</p> <p>The temperature of the PV cell was maintained below 40 °C, which extended the working time of the PV cell close to the rated power (3.5–4 h), and outputted 7.9% more electricity.</p>	[76]
PV-PCM	Beef tallow–coconut oil–paraffin	<p>A novel PCM composite is introduced for thermal management of a PV module.</p> <p>Mixture of beef PBT CO is used as an efficient PCM.</p> <p>Increasing thermal conductivity of PBT CO using EG particles.</p> <p>Temperature of PV module is reduced from 64.04 °C to 32.92 ssd by 9.94% wt EG/PBT CO.</p> <p>The maximum efficiency of the PV–EG/PBT CO system at the optimum point is 14.89%.</p>	[77]
PV-PCM	Paraffin	<p>During the late melting period, it was discovered that the composite PCM experienced a significant decrease in its melting rate, resulting in the formation of a prolonged solid PCM region known as the “dead zone”.</p>	[78]
PV-PCM	Gallium and paraffin	<p>Dynamic melting was characterized by a pore-scale lattice Boltzmann model.</p> <p>Selection of PCM for PV thermal management was studied.</p> <p>A low melting temperature offers a quick response but with a short duration.</p> <p>A high latent heat offers high energy density while taking a long time to melt.</p>	[79]

**Table 9.** Continued.

System types	PCMs	Highlights	Reference
PV-PCM	Paraffin	A novel cooling system of PV module employing PCM nanoemulsion was presented. PCM nanoemulsion possessed a low supercooling degree and high apparent specific heat. Lower temperature and higher output power of PV module was obtained via using PCM nanoemulsion. PCM nanoemulsion required less pumping power consumption compared with the water-cooling system. The effects of the supercooling degree on the cooling performance were investigated.	[80]
PV-PCM	Paraffin	PV temperature can be reduced by 19 °C by using PCM. Effects of operating conditions on the performance of system are analyzed. Increase in tilt of system leads to increase in rate of heat extraction by PCM.	[81]
PV-PCM	Paraffin	Energy storage with PCM used below PV cells was studied in presence of metal foam. Metal foam and inclination angle effects on PV efficiency and PCM energy storage were studied. Increment of inclination angle improves the efficiency. Using high porosity metal foams enhances the PCM conductivity and melting time. Using metal foams causes reduction in thermal storage capacity.	[82]
PV-PCM	Paraffin	Optimum depths of PCM container for various fin dimensions were computed. Optimum fin dimensions were computed to maintain PV at low temperature. Optimum depths were computed for various levels of daily solar radiation too. Best spacing between successive fins is 25 cm.	[83]
PV-PCM	Paraffin	Power production from fins-fitted system was computed for a range of enclosure depths. Best depth of fins-fitted enclosure computed for various working circumstances. Influence of wind pace and azimuth, surrounding temperature, and melting point studied. Influence of successive fins distance, fins depth, and fins width was evaluated.	[84]
PV-PCM	Not mentioned	Duration of power improvement of PV by fin PCM was reported. Consequence of azimuth and flow rate of wind on working of PV with fin PCM was studied. Effect of fin PCM volume on duration of power improvement was studied.	[85]
PV-PCM	Paraffin	Duration of power improvement of PV by fin PCM was reported. Consequence of azimuth and flow rate of wind on working of PV with fin PCM was studied. Effect of fin PCM volume on duration of power improvement studied.	[86]
PV-PCM	Paraffin	Decrease in tilt of PCM container from 45° to 0° reduced charging efficiency by 32%. Decrease in tilt of PCM container to 0° reduced rate of energy storage to $180 \text{ W m}^{-2}$ .	[87]
PV-PCM	Petrolatum	A new type of heat sink made up of drilled cylindrical rods and PCM was used to investigate thermal management of PV module. The proposed model was investigated both experimentally and by using numerical simulations. The impacts of air velocity and incidence angle of air on heat dissipation from the module were evaluated. The average temperature of the PV module has dropped by 5.18 °C.	[88]
PV-PCM	Paraffin	The PV-PCM efficiency is improved by 2.9%, and the output voltage is increased by 0.53 V. A numerical study of PCM layer attached behind PV cell was performed. Phase-change process of a PCM was studied under Tunisian climate. $9 \text{ g m}^{-2}$ of dust deposition reduces PV cell power output of about 3 W at midday. Wind direction increase from 30° to 60° rises PV cell temperature from 64 to 69 °C.	[89]
PV-PCM	Not mentioned	As wind speed drops from 6 to $0.2 \text{ m s}^{-1}$ , increase in power elevates from 12 to $23 \text{ W m}^{-2}$ . As wind angle of approach drops from 75° to 0°, increase in power drops 18 to $14 \text{ W m}^{-2}$ . As ambient temperature rises to 289–299 K, increase in power elevates to 16–21 $\text{W m}^{-2}$ . As liquefaction temperature rises to 291–301 K, enhancement period rises to 6.5–12 h.	[90]
PV-PCM	$\text{CaCl}_2 \cdot 6\text{H}_2\text{O}$	PCM was used to cool two-axis tracking PV cells. Experiments showed temperature distribution of PCM during melting and solidification. The PCM increased the efficiency of PV cell by approximately 7% in a mild climate. Higher efficiency increases are expected in hot climates for utility scale PV plants.	[91]

**Table 9.** Continued.

System types	PCMs	Highlights	Reference
CPV–PCM	$\text{Al}_2\text{O}_3\text{-CaCl}_2\cdot 6\text{H}_2\text{O}$	Nanoparticle–PCM enhances temperature uniformity and efficiency of solar cells. Increasing nanoparticle fraction in PCM reduces local solar cell temperature. Using $\text{Al}_2\text{O}_3$ –PCM is a more effective cooling method compared to $\text{SiO}_2$ or $\text{CuO}$ .	[93]
CPV–PCM	Paraffin	Maximum temperature reduction is obtained as 20 °C with NEPCM.	[94]
CPV–PCM	n-octadecane paraffin (PCM1), calcium chloride hexahydrate $\text{CaCl}_2\cdot 6\text{H}_2\text{O}$ (PCM2), and a eutectic mixture of capric–palmitic acid (PCM3)	Power output and energy efficiency are improved by 7% and 6% respectively with PCM. Performance of CPV cell improves with addition of graphene nanoplatelets in PCM. A comprehensive transient melting–solidification–thermo-fluid model was developed. Using five parallel cavities attained the highest reduction of cell temperature. PCM arrangements affect the solar cell temperature uniformity.	[95]
CPV–PCM	Paraffin	CPV-integrated PCM system has been developed in COMSOL Multiphysics. Effects of fill volume of PCM and CR have been studied on PCM temperature. A significant reduction in CPV temperature is observed with addition of PCM. CPV temperature is maintained constant during the melting period of the PCM. CPV module power output and efficiency increase with increase in PCM fill volume.	[96]
CPV–PCM	Paraffin	The suggested configurations improve the heat transfer and PCM melting processes.	[97]
BIPV–PCM	n-octadecane NePCM	Remarkable energy management enhancement is observed in the PV system using PCM encapsulation. A numerical simulation of NePCM coupled with BIPV has been conducted.	[100]
BIPV–PCM	70 wt% $\text{Na}_2\text{SO}_4\cdot 10\text{H}_2\text{O}$ + 30 wt% $\text{N}_2\text{O}_6\text{Zn}\cdot 6\text{H}_2\text{O}$	The BIPV/NePCM system restricts the cell's temperature rise below 40 °C for about 60 min. Cu is more effective in cooling as compared to $\text{CuO}$ , $\text{Al}_2\text{O}_3$ , and $\text{TiO}_2$ nanoparticles. The two inorganic PCM was characterized to form eutectic PCM. The optimum molar ratio of 70 wt% $\text{Na}_2\text{SO}_4\cdot 10\text{H}_2\text{O}$ and 30 wt% $\text{N}_2\text{O}_6\text{Zn}\cdot 6\text{H}_2\text{O}$ . PCM improved output power of BISTPV module from 34 287 to 37 024 W year <sup>-1</sup> . The new method was devised to incorporate the PCM in BISTPV modules.	[101]
BIPV–PCM	$\text{Na}_2\text{SO}_4\cdot 10\text{H}_2\text{O}$	Simplified BIPV–PCM system has been developed. Novel method has been proposed to incorporate the inorganic hydrated salt PCM. Incorporation of PCM improved the electrical efficiency by 10%. The BIPV–PCM cell temperature is reduced up to 8 °C compared to reference module. Suitability of BIPV–PCM for facades at various orientations is investigated.	[102]
BIPV–PCM	Paraffin	The thermal and electrical performance of a building was studied. The peak demand load is reduced by maximum of 47% using 5.2 vol% PCMs. Three optimizations are conducted to realize the maximum economic benefits. Carbon emissions are reduced by 11.58 kg using 5.2 vol% PCMs in a 6.25 m <sup>2</sup> building.	[103]
BIPV–PCM	Docosanol	With the exception of scenario 1, all scenarios assumed PV equipment installed on the roof surface. PCM was used on the back of the PV cell in scenario 3, while scenario 4 involved the addition of a brick layer infused with PCM to the roof surface. In scenario 5, the techniques of scenario 3 and scenario 4 were combined and applied. By installing PV cells to generate electricity, energy saving was achieved, and the overall load reduction rate was up to 22.55%.	[104]
PV–TE–PCM	Paraffin	The minimum payback period calculated is 7 years, which is reasonable. Different methods were used to maintain PV at low temperatures. Results compare the amount of temperature, efficiency, and power generation enhancement. The PV cell's temperature control simulations are compared with different models at fair and sunny weather conditions. The addition of PCM module does not enhance the system performance.	[105]

**Table 9.** Continued.

System types	PCMs	Highlights	Reference
PV–TE–PCM	Paraffin	<p>Energy efficiency of the CPV–TE system is 46.5% higher than that of the CPV–PCM system.</p> <p>Different configurations of hybrid-cooled CPV systems result in different performances.</p> <p>Energy efficiency of the CPV–TE–PCM system is 2.4% higher than that of the CPV–PCM–TE system.</p> <p>Melting temperature of a PCM should be a few degrees higher than the ambient temperature.</p> <p>Cross-fin configuration of the PCM container enhances heat transfer from the rear side of the PV to the PCM.</p>	[106]

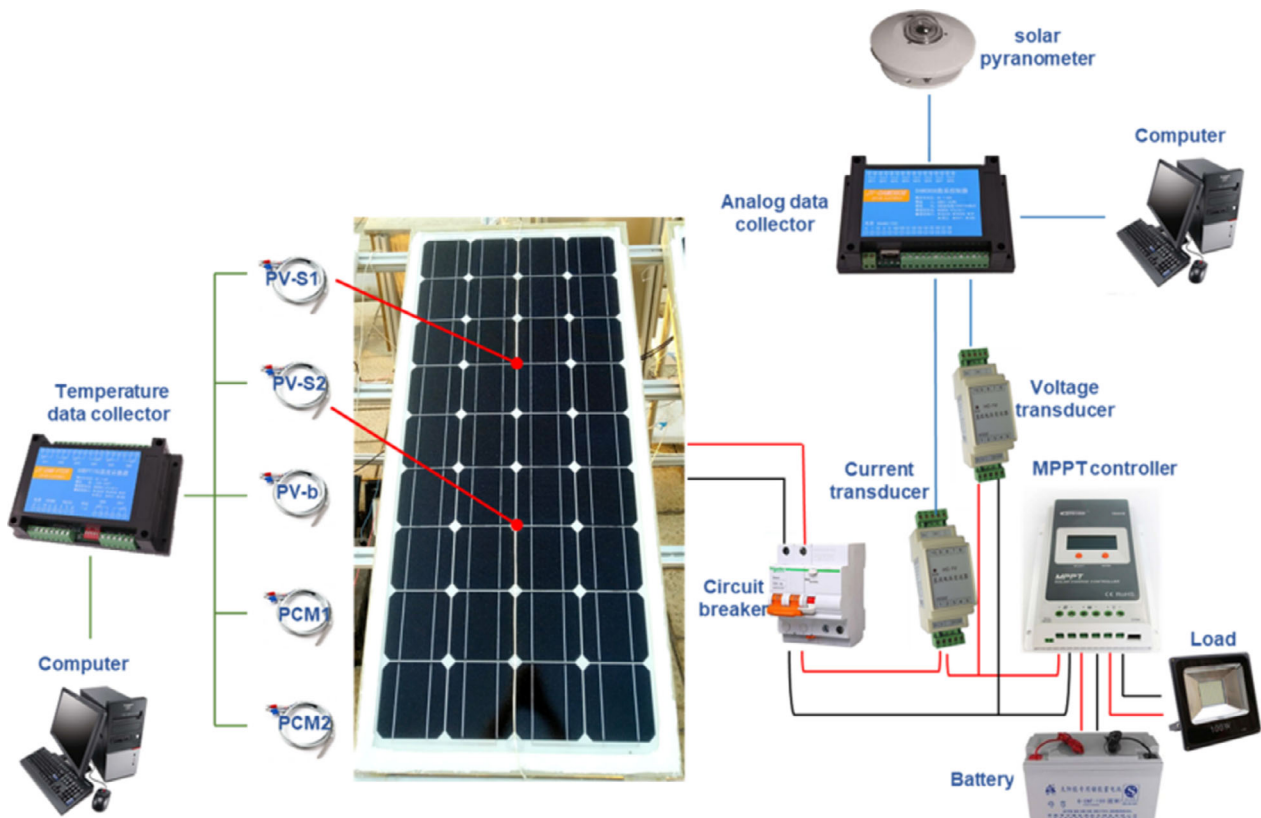


**Figure 21.** Optimization and inspection of the performance of PV–PCM systems on a seasonal and yearly basis using experimental design.

**Table 10.** Thermal conductivity of commonly used cooling medium.

Cooling medium	Thermal conductivity [ $\text{W m}^{-1} \text{K}^{-1}$ ]
Air	0.0259
Water	0.6065
Ethylene glycol	0.2539

panel temperature to 4.3, 3.4, 3.6, and 3.7 °C in the natural flow mode, forced high speed mode, medium speed mode, and low speed mode, respectively. Furthermore, decreasing the temperature can enhance the power output and electrical efficiency. Kanzari et al.<sup>[110]</sup> created a digital PV/T-PCM system in a

MATLAB environment. The productivity of PCM integrated in PV/T air panels was evaluated through simulations using the optimized model. **Figure 22** illustrates the heat transfer diagram of the PV/T-PCM system model. The simulation outcomes are pleasing and can be extended to other categories of panels where PCM can be positioned. Sohani et al.<sup>[111]</sup> determined the optimal thickness of PCM using a multi-objective optimization (MOO) technique that takes into account the performance of real-time data throughout the year. By considering objective functions such as annual energy storage (AES), AEP, PBP, leveled cost of energy (LCOE), and annual carbon-dioxide reduction (ACDR), a favorable situation was achieved. An illustration of a residential structure in Tehran, Iran, was utilized to employ numerical simulation, and a combination of technique for order preference by similarity to an ideal solution (TOPSIS) and

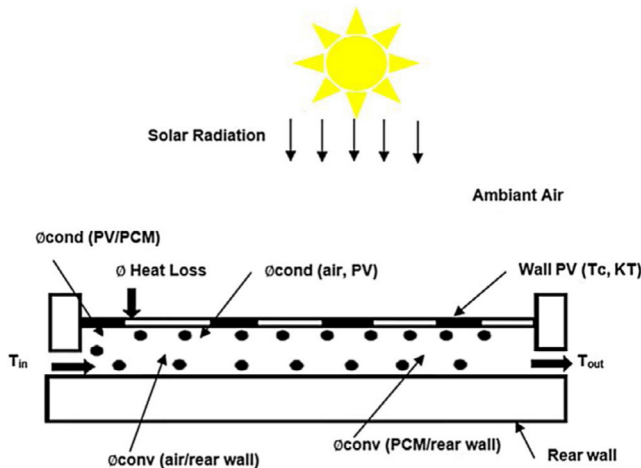


**Figure 22.** Heat exchange of air panel in PV/T-PCM system.

non-dominated sorting genetic algorithm II (NSGA-II) methods was employed to ascertain the ultimate optimal resolution. According to the findings, the most suitable PCM thickness measures 77.2 mm. The utilization of PCM with the ideal thickness resulted in a significant enhancement of AES, AEP, ACDR, and LCOE by 22.24%, 9.93%, 17.69%, and 9.59%, respectively, in comparison to solely relying on air thermal management. The PBP under optimal conditions is 3.321 years, indicating the economic feasibility of using MOO.

#### 4.2. Water-Cooled PV/T-PCM Systems

Table 9 shows that water has a better heat transfer capacity than ethylene glycol. Additionally, the operating temperature of PV thermal management is significantly below the boiling point of water. Therefore, water is widely used as the main liquid cooling medium in PV/T-PCM systems.

The inclusion of water-cooled tubes increases the packaging requirements of PCM for water-cooled PV/T-PCM systems. Fu et al.<sup>[112]</sup> used microencapsulated PCM (MPCM) slurry as the cooling medium to establish a water-cooled PV/T-PCM experimental system. The schematic diagram of the system can be seen in **Figure 23**. A study was conducted on the overall efficiency of a PV/T-MPCM system that utilizes water-cooling. A comparison was made between the electrical efficiency and thermal efficiency of a PV/T-MPCM system with water-cooling, using MPCM grout and tap water, under various operating conditions. A comparison is made between the real-life performance of a conventional water-cooled PV/T system and a similar system incorporating a PCM layer. The results showed that the MPCM mixture can reduce the temperature of PV cells and improve the TE efficiency of PV cells. PV/T systems that utilize MPCM slurps outperform those that utilize pure water or water with PCM layers. The system witnessed a notable enhancement of 0.8% in its average electrical efficiency and a substantial increase of 13.5% in its maximum thermal efficiency. To solve the leakage problem of PCM and improve its thermal conductivity, Ahmadi et al.<sup>[113]</sup> added polystyrene–CNT (PS–CNT) foam to PCM to achieve shape stability. Then, passive and active cooling

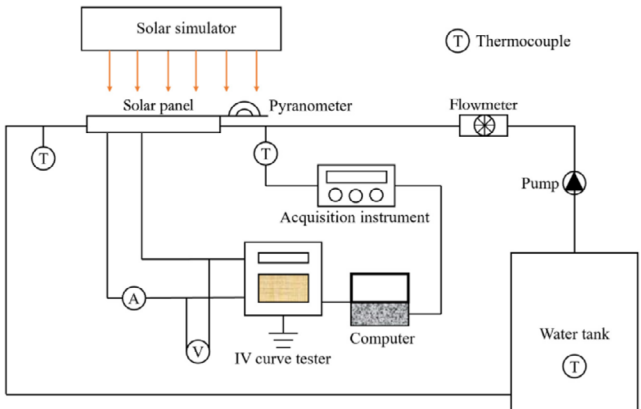


**Figure 23.** Schematic diagram of water-cooled PV/T-MPCM experimental system.

experiments were carried out to study the effect of PS–CNT foam PCM on the TE efficiency of the PV/T-PCM system. The solar simulator was utilized for conducting all experiments, with a power range of solar radiation between 800 and 1700 W m<sup>-2</sup>. According to the findings, the integration of PCM was found to lower the temperature of PV cells by 6.8% while simultaneously enhancing the electrical efficiency by 14.4%. The PV/T-PCM system achieves significantly higher performance compared to the pure passive PV-PCM system due to its efficient power generation and heat harvesting, resulting in an energy efficiency range of 66.8–82.6%.

The addition of nanoparticles to PCMs can improve the thermal conductivity of water-cooled PV/T-PCM systems and promote heat transfer between PV cells and PCMs, as well as between PCMs and the liquid working medium. Consequently, the TE efficiency of PV/T-PCM systems experiences a substantial enhancement. Islam et al.<sup>[114]</sup> used NePCM to improve the TE characteristics of PV/T system. In Malaysia, simultaneous outdoor experiments were conducted to study five distinct systems, which include PV, PV/T, PV-PCM, PV/T-PCM, and PV/T-NePCM, in real-time climate conditions. **Figure 24** displays the apparatus used for the experiment. The trial was conducted at a range of 0.5–4.0 L min<sup>-1</sup> flow rate. A digital data acquisition system was used to record the real-time measurements of ambient temperature, air humidity, wind speed, and fluid flow. The system's performance was evaluated using the energy method and the exergy method. The findings indicated that the PV/T-NePCM system experienced a temperature rise exceeding 46 °C in the effluent. The maximum overall energy efficiency of the system is 85%. Abdullah et al.<sup>[115]</sup> conducted an experimental study based on the efficiency of plate solar stills (SS). **Figure 25** displays the tested SSs, including the flat trays SS, corrugated trays SS (CTSS), and conventional SS (CSS). To enhance the performance of CTSS, an experiment was conducted using a combination of PCM and CuO nanoparticles. Furthermore, the water was heated using three electric heaters. Energy is directly drawn by the heater from the PV module. The PV components are directly mounted on the rear side of the SS, effectively utilizing the identical space of the SS. According to the experimental findings, the total amount of fresh water produced

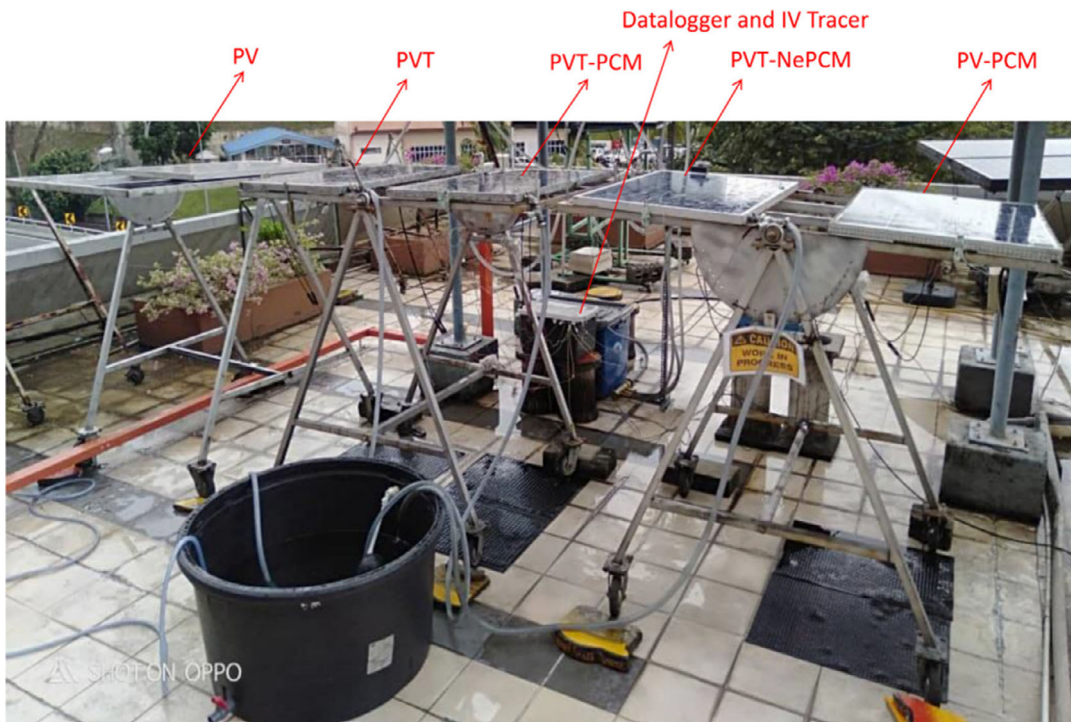


**Figure 24.** Experimental device for performance comparison of five kinds of systems.



**Figure 25.** Pictorial view of tested solar stills: a) conventional solar still, b) trays solar still, and c) corrugated trays solar still.

by CTSS with an electric heater is raised by 150% compared to CSS, while CTSS with NePCM shows a 122% increase in fresh water yield. In addition, when using corrugated absorbers, NePCM, and electric heaters, CTSS increased its total water production by 180% compared to CSS.

The main objective of the aforementioned studies is to enhance the TE efficiency of a water-cooled PV/T-PCM system through the modification of PCMs. There are two main categories of research on the practical use of water-cooled PV/T-PCM system. The first category is the integration of PV/T-PCM with buildings, known as BIPV/T-PCM system. The second category is the introduction of CPV, known as CPV/T-PCM system.

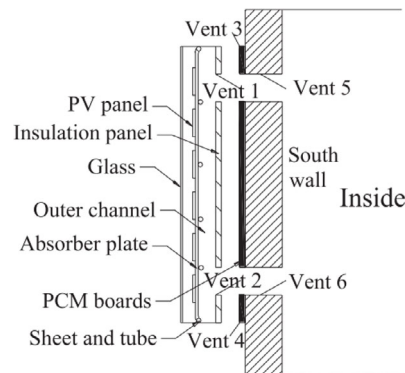


**Figure 26.** Schematic diagram of double-duct solar wall system.

The dual-ducted solar wall system provides electricity and heat to the building through a water-cooled PV/T-PCM system. It is a typical example of BIPV/T-PCM application research. The ultimate goal of BIPV/T-PCM systems is to achieve zero energy consumption in building structures. Xu et al.<sup>[116]</sup> proposed a hybrid PV/T solar wall system in an area with four distinct seasons. The fundamental concept of the system, as depicted in Figure 26, at night, in addition to reducing the cooling load in summer and the heat load in other seasons, produces electricity and hot water (or air) to decrease the energy burden of the building both during the day and night. Experiments were conducted continuously throughout the day in three different seasons: summer, winter, and the transition season. During the period of seasonal change, there was a decrease in the daytime cooling demand and the nighttime heating demand. In winter, the electrical efficiency

reached 12.3%, the temperature rose by 10.8 °C during the day and 1.4 °C at night. During the summer season, the electrical efficiency and thermal efficiency stood at 10.2% and 57.3% correspondingly. Throughout the day, the indoor temperature was 1.2 °C lower than the reference room during the day and 0.5 °C lower at night, resulting in a decrease in the cooling load. Following the above research, Ke et al.<sup>[117]</sup> investigated the performance of the hybrid PV/T solar wall system and selected Urumqi, Beijing, and Hefei as the sites to study its annual performance. The annual power generation of the three cities was 179.67, 179.21, and 119.28 kWh, respectively. The average electrical efficiency was 11.22%, 10.67%, and 11.06%, respectively.

Section 3 of this article describes how CPV can improve the efficiency of solar energy and cause the temperature of PV cells to rise. Compared with CPV–PCM systems, CPV/T-PCM systems can not only increase the power generation of PV cells, but also increase the water temperature collected by cooling water. Hence, in situations where there is a high need for heat, CPV/T-PCM systems offer distinct benefits compared to PV/T-PCM systems. Karaac et al.<sup>[118]</sup> conducted an experimental study on CPV/T solar dryer using NePCM ( $\text{Al}_2\text{O}_3$ -paraffin). Figure 27 displays the solar dryer. The components of the system include a concentrator, a PV cell, a solar gel cell, a charge regulator, a data logger, an aluminum flexible tube, fans, a cover, and a greenhouse. According to the principle of the first and second law, the thermodynamic analysis of the system is carried out. Furthermore, the drying parameters were predicted using two machine learning algorithms, namely artificial neural network (ANN) and support vector machine (SVM). To compare the success rate of predictions, we utilized various metrics including  $R^2$  (coefficient of determination), relative root mean square error, mean absolute error (MBE), and relative MAE. The system has an overall thermal efficiency of 20% and an exergy efficiency of 8%. Although the solar radiation to the environment was much reduced, the heat energy transferred to the NePCM prevented the greenhouse temperature from falling for the first 100 min. Within this system, the mushrooms undergo dehydration, reducing their original moisture level of 17.45 g water  $\text{g}^{-1}$  dry matter to a concluding moisture level of 0.0515 g water  $\text{g}^{-1}$  dry matter. The rate at which the system dries is 0.436 g matter  $\text{g}^{-1}$  dry matter·min $^{-1}$ . Kong et al.<sup>[119]</sup> constructed a composite parabolic CPV/T-PCM system, as shown in Figure 28. Various factors were examined in an outdoor environment. Throughout the experiment, as the solar irradiance and ambient temperature varied, the PCM transitioned from a solid state to a melted state. Consequently, the temperature nonuniformity coefficient of the PV module/PCM decreased from 4.28/1.34 to

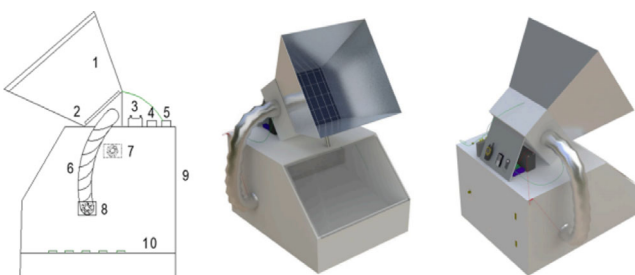
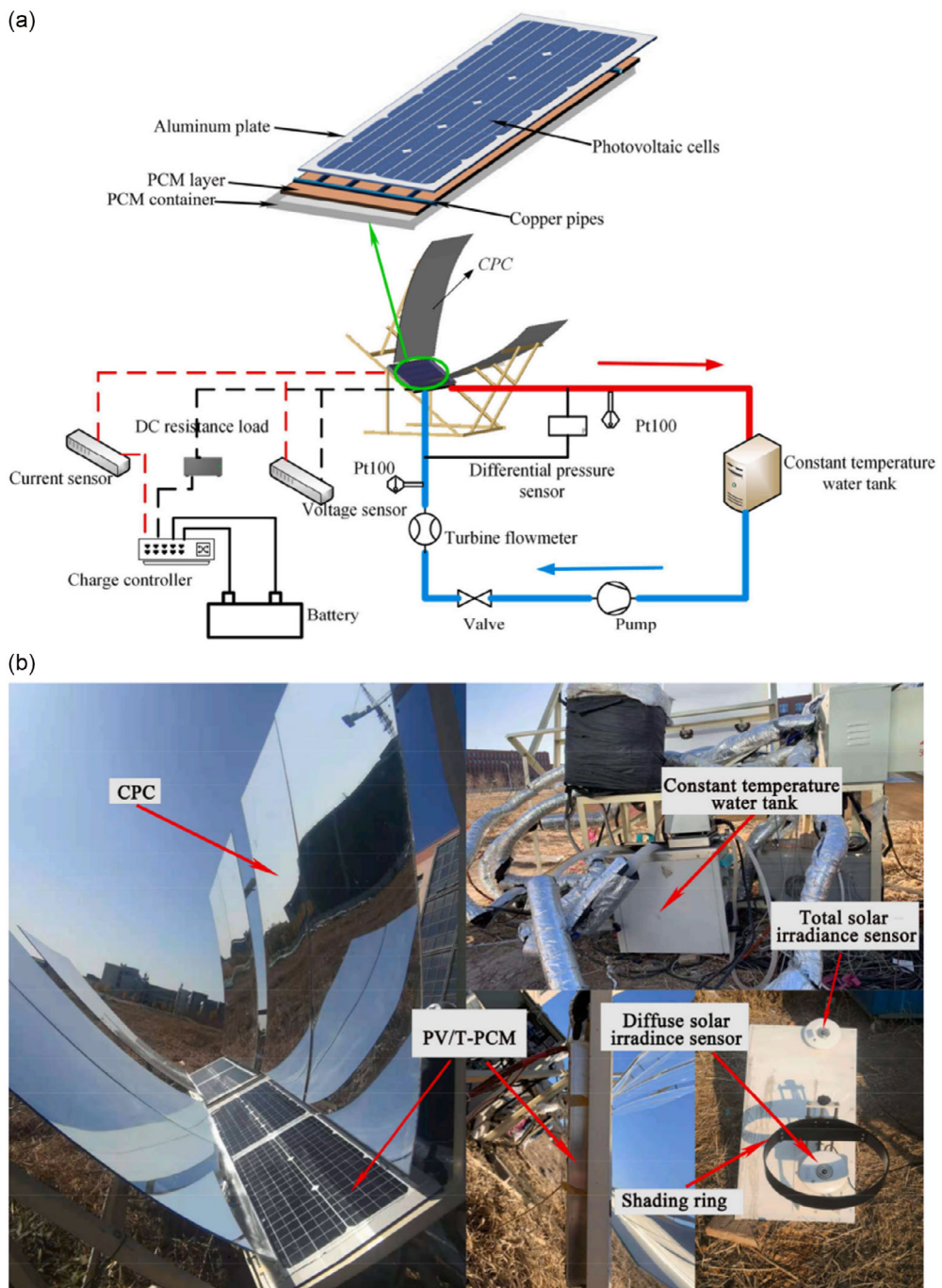


Figure 27. Schematic diagram of solar dryer.

1.42/0.66, clearly demonstrating the substantial enhancement of temperature distribution uniformity achieved by the PCM. Setting the pump state to OFF–ON–OFF resulted in an initial increase in the PV module temperature from 10.6 to 33.2 °C, followed by a rapid decrease to 28.5 °C, and finally a gradual decrease to 27.1 °C. This demonstrates that the utilization of PCM and liquid cooling effectively lowers the temperature of the PV module. While the pump was in operation, the thermal efficiency, electrical efficiency, and primary energy efficiency experienced a decline from 19.6% to 5.0%, 4.8% to 3.0%, and 30.4% to 16.8%, respectively. The average values for these efficiencies were 7.1%, 4.0%, and 17.6%. The CPV/T-PCM system exhibits superior cogeneration performance, with a maximum primary energy efficiency that is 7.9% higher compared to the CPV system alone.

It is important to optimize the heat transfer structure of water-cooled PV/T-PCM system. At present, there is little research on this, so this is bound to be a major area of interest for future researchers. Kazemian et al.<sup>[120]</sup> developed a predictive model using the RSM. The established water-cooled PV/T-PCM model is shown in Figure 29. The study focused on investigating the correlation between the independent parameters, which are the operating factors, and the relevant parameters, which are important response factors, of the water-cooled PV/T-PCM system. PCMs considered were RT series organic PCMs. RSM was utilized for both single objective and MOO, taking into account various optimization goals, and providing recommendations for the optimal values of control factors in different operational scenarios. Factors considered for analysis were the thickness of the PCM layer, solar radiation, the melting temperature of the PCM, and the surrounding ambient temperature. A diagnostic analysis was conducted for each response to evaluate the statistical sufficiency of the model and demonstrate its reasonable accuracy in prediction. The recommended model was evaluated using analysis of variance and perturbation analysis to assess its applicability and statistical significance. The findings indicated that solar radiation has a greater impact on energy and exergy output compared to other operating factors. To optimize TE utilization while minimizing entropy production, the PCM layer thickness is set to 1.5 cm. El-Hamid et al.<sup>[121]</sup> conducted a 3D numerical simulation and comparative analysis of glazed and unglazed PV/T structures. The structures were evaluated both with and without the use of PCM, as well as with PCM placed at various locations. Figure 30 shows a schematic of the constructed structural models. Six variations of the PV/T or PV/T-PCM structure were designed, water pipes were added to the PCM, and both glazed and unglazed options were adopted. The energy and exergy of six arrangements were evaluated and compared to determine their performance. The effects of coolant flow were assessed in laminar and turbulent regions, and daily CO<sub>2</sub> emissions were assessed. The findings indicated that the inclusion of the water conduit within the PCM framework beneath the PV/T module can greatly enhance the overall efficiency. Furthermore, the unglazed elements generate a slightly greater amount of electrical power compared to the glazed element. In the proposed design, the glazed water-cooled PV/T-PCM systems achieve the highest average daily energy, while the unglazed systems achieve the highest energy efficiency.



**Figure 28.** CPV/T-PCM system: a) composite parabola diagram and b) photograph.

#### 4.3. Nanofluid PV/T-PCM Systems

The TE efficiency of PV/T-NePCM systems is greatly enhanced as a result of the superior thermal conductivity of NePCMs. Likewise, the introduction of nanomaterials into the cooling water of a water-cooled PV/T-PCM system can enhance the thermal conductivity of the water, thereby improving the TE efficiency of the entire system. Jidhesh et al.<sup>[122]</sup> designed a

semitransparent PV-T hybrid collector (SPV-THC). It was then tested in Coimbatore, India, to verify its usefulness. Figure 31 shows the SPV-THC system. The system consists of a transparent polycrystalline silicon PV module with a winding tube structure containing water and nanofluids to capture heat energy from the PV module. The nanofluid consists of 0.2 vol% CuO. The nanofluid had a mass flow rate of  $0.016 \text{ kg s}^{-1}$  after optimization. PCM made from a combination of paraffin and talc was utilized.

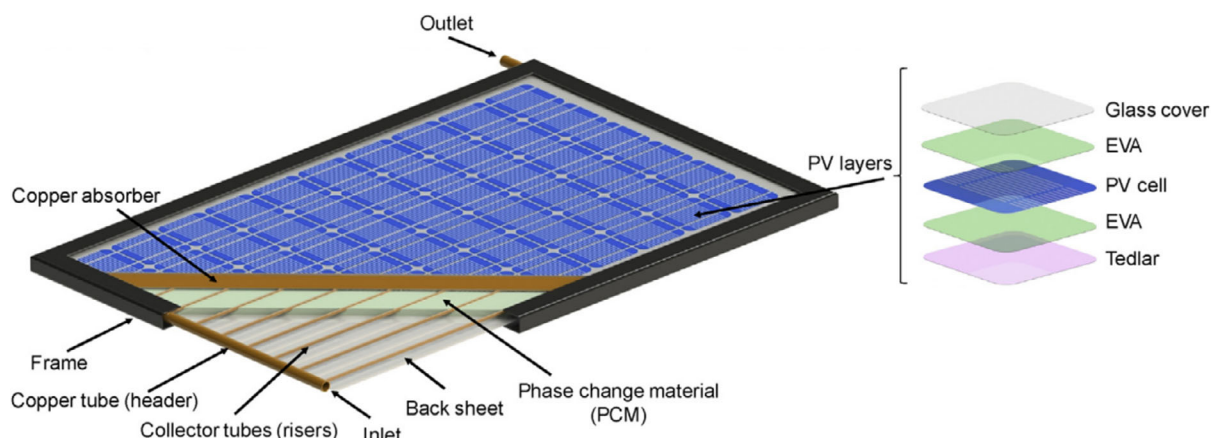


Figure 29. The 3D water-cooled PV/T-PCM model.

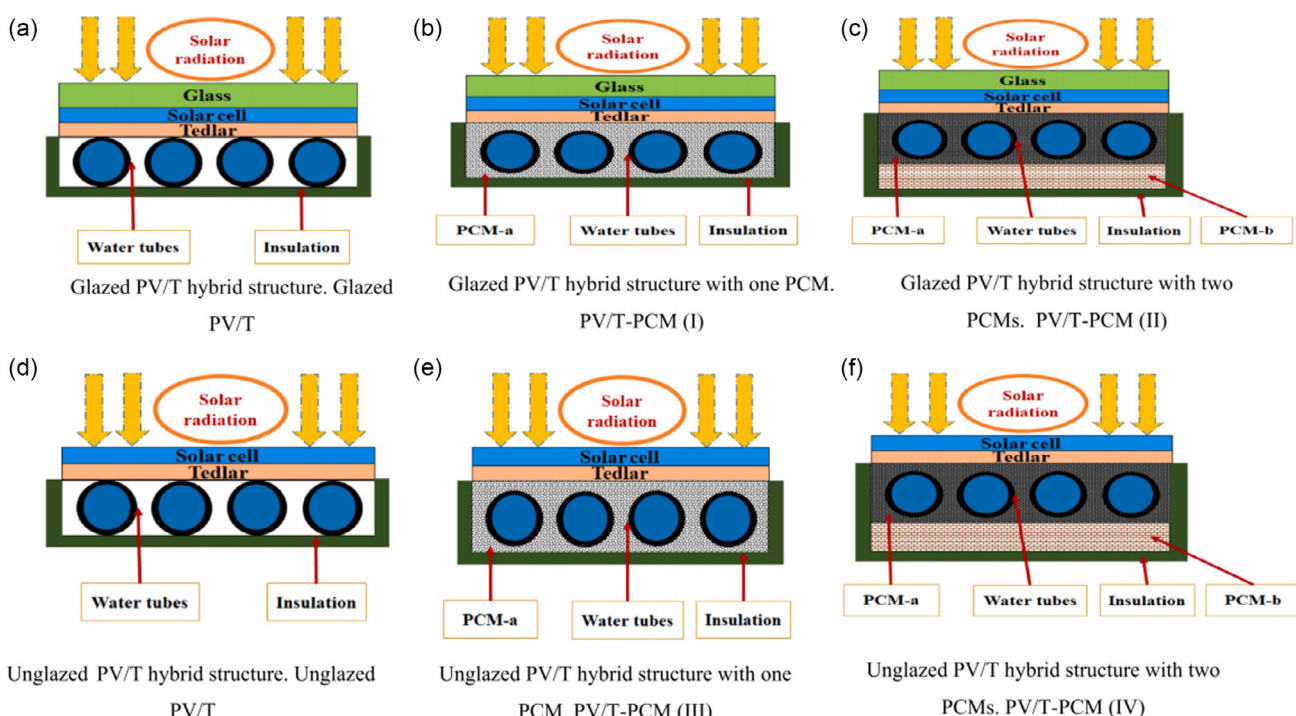
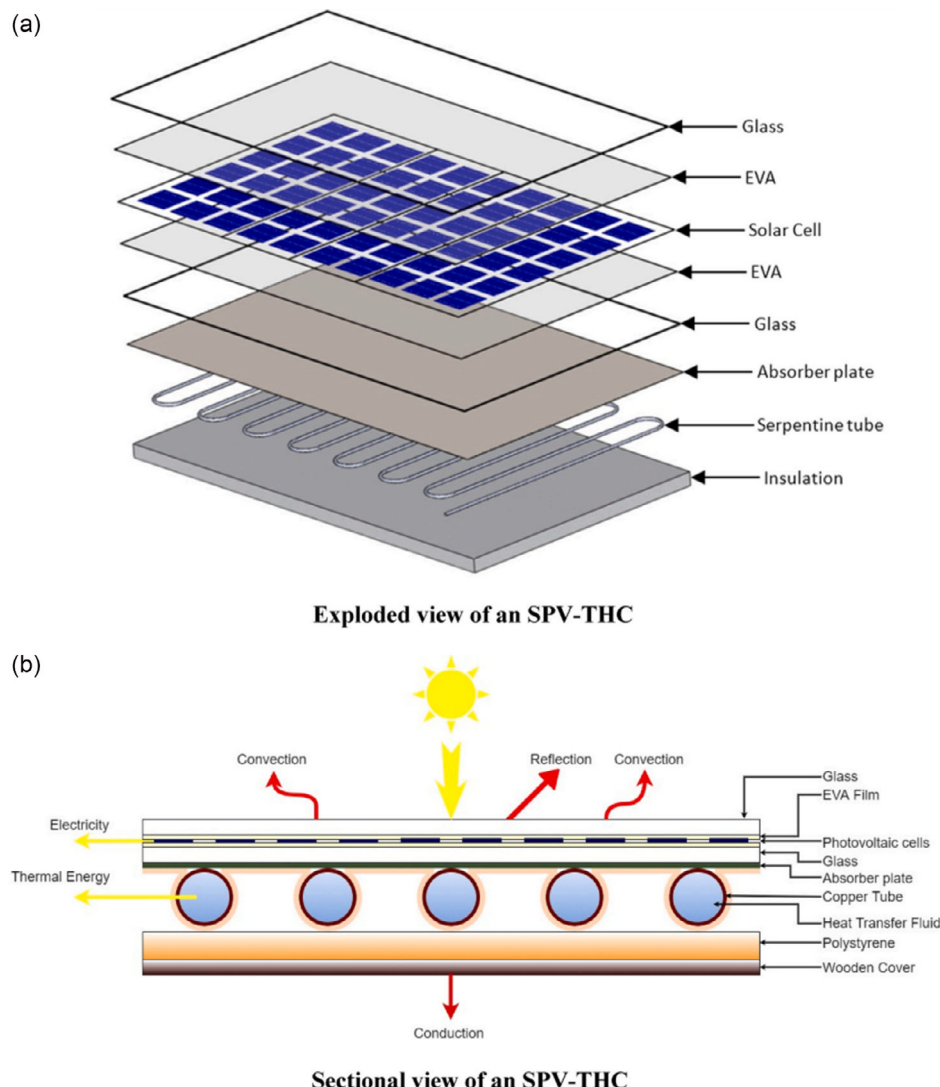


Figure 30. Six variants of PV/T or PV/T-PCM structure, with both glazed and unglazed options: a) glazed PV/T: glazed PV/T hybrid structure; b) PV/T-PCM (I): glazed PV/T hybrid structure with one PCM; c) PV/T-PCM (II): glazed PV/T hybrid structure with two PCMs; d) unglazed PV/T: unglazed PV/T hybrid structure; e) PV/T-PCM (III): unglazed PV/T hybrid structure PV/T hybrid structure with one PCM; and f) PV/T-PCM (IV): unglazed PV/T hybrid structure with two PCMs.

The thermal model was established by energy balance equation and verified by experimental analysis. According to the experimental findings, the system experienced an average cooling effect of 9 and 12 °C when using water and CuO nanofluids, respectively. Compared to conventional opaque PV components, CuO nanofluids and water exhibited an increase in electrical efficiency of 11.2% and 5.9%, respectively. The CuO nanofluid system exhibited a thermal efficiency that was 43% greater than the water system. Furthermore, the SPV-THC-PCM system exhibited a remarkable enhancement in exergy efficiency, with

a 26% and 12.25% increase when utilizing CuO nanofluids and water, respectively, in contrast to conventional PV systems. Rahamanian et al.<sup>[123]</sup> integrated a new PCM radiator with a building-integrated CPV system. To enhance thermal conductivity, the PCM was enclosed in an aluminum casing within a nano-fluid reservoir. The TE performance of the system was evaluated using a validated and simulated comprehensive numerical model, considering both passive and active cooling conditions. The melting and solidification process of PCM under CR5 was studied. Passive cooling effectively keeps the temperature



**Figure 31.** Exploded and sectional details of an SPV-THC: a) exploded view of an SPV-THC and b) sectional view of an SPV-THC.

of CPV below 78 °C. Furthermore, with the implementation of active cooling, the PV cell's temperature was effectively regulated to remain below 43 °C, ensuring a consistent distribution throughout. The enhanced thermal conductivity and natural convection of the nanofluids within the PCM container are the primary factors contributing to this performance improvement. Khodadadi et al.<sup>[124]</sup> carried out a numerical study on the improved PV/T linear Fresnel mirror (PV/T-LFR) with the integrated NePCM technology. Figure 33 displays the diagram of the PV/T-LFR system with NePCM and its modeling flow chart. The performance of the collector was assessed by examining the impacts of varying mass flow rates and the inclusion of Al<sub>2</sub>O<sub>3</sub> nanoparticles in both the cooling water and PCM. A transient solver was selected to model the PV/T-LFR system. Computation fluid dynamics (CFD) method was used to solve the governing equation of PV/T-LFR. A basic algorithm was employed to connect velocity and pressure. The findings indicated that decreasing the mass flow rate and incorporating nanoparticles into PCM lead to a decrease in the system's electrical

efficiency, whereas the system's electrical efficiency is enhanced by introducing nanoparticles into the cooling water. The system's thermal output rises as the mass flow rate increases. Furthermore, the inclusion of nanoparticles in both the cooling water and PCM yields a beneficial impact on the collector's heat output **Figure 32**.

The study found that incorporating nanoparticles into PCM resulted in a decrease in the electrical efficiency of the system, whereas introducing nanoparticles into the cooling water led to an increase in the electrical efficiency of the system. Although nanoparticles enhance the thermal conductivity of PCMs, they do so to a certain extent at the cost of reducing latent heat. According to Khodadadi's findings, the addition of nanoparticles to cooling water yields superior results compared to adding nanoparticles to PCM. However, there are not enough theoretical and experimental studies to confirm this conclusion. This is not only valuable for the research and development of nanofluid PV/T-PCM systems, but also crucial for the practical application of nanomaterials. Therefore, this is bound to be the focus of future research.

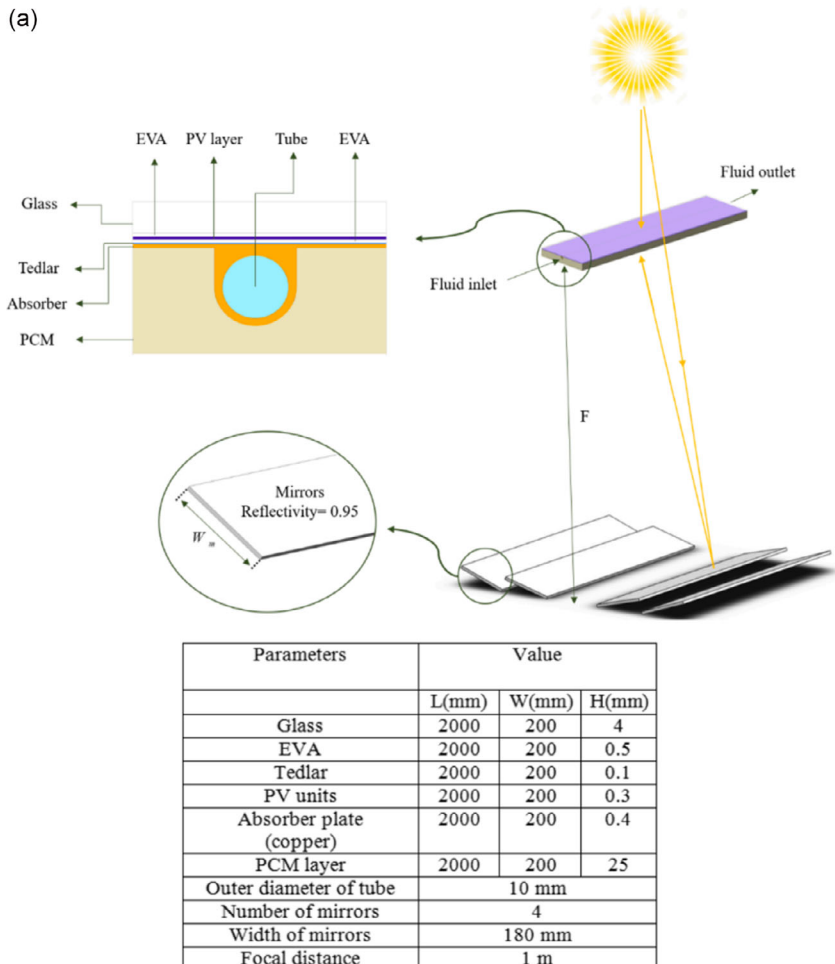


**Figure 32.** a) PV/T-LFR system with NePCM and b) modeling flowcharts.

#### 4.4. Coupling of PV/T-PCM System and Heat Pump

PV cell cooling and PV/T system heat collection is contradictory. The better the PV cell cooling effect often means the less heat collection. Since the grade of electrical energy is higher than the heat energy, the PV/T system gives priority to the electrical efficiency, and the improvement of the heat collection efficiency of the coolant is considered after the electrical efficiency of the

system reaches the actual requirements. Therefore, the temperature of the coolant collection is often 30–40 °C, barely reaching the temperature of domestic hot water, and for scenes with high temperature requirements in industrial use (such as absorption refrigeration, seawater desalination, etc.), the temperature of the coolant collection is not enough. At this point, it is advisable to couple the PV/T-PCM system with a heat pump to provide a higher water temperature. Kosan and Aktaz<sup>[125]</sup> designed

and manufactured a new type of latent heat storage system integrating (dual-channel) PV/T with heat pump condenser. The physical device of the system is shown in **Figure 33**. The thermal behavior of PCM in latent heat storage unit was numerically analyzed by using Ansys Fluent software. The maximum average electrical and thermal efficiency of PV/T-PCM and heat pump systems is 16.74% and 66.98%, respectively. The results showed that the average performance coefficient of the heat pump system is between 2.93 and 3.18. The PV/T-PCM system is capable of storing 1.07 kWh of electricity, producing 9.59% more power than a single PV cell. The melting time of paraffin wax is 183–201 min, and the solidification time is 348–357 min. The melting and solidification time vary with the performance of the heat pump. Ren et al.<sup>[126]</sup> investigated the energy flexibility

of a net-zero energy house using a solar-assisted air-conditioning system with integrated thermal energy storage and demand-side management (DSM) strategy, as shown in **Figure 34**. A total of 40 alternative designs for solar-assisted air-conditioning systems were developed, along with four DSM strategies, including over-heating/cooling, preheating/cooling, temperature set point relaxation, and heat pump charging. The results showed that using the DSM strategy, the heat pump solar contribution (i.e., the ratio of energy consumption provided by PV to total energy consumption) is 0.79. The use of PCM units can further increase the contribution of solar energy to nearly 1.0. When charging with superheat/cooling and/or heat pumps, temperature set point relaxation and superheat/cooling strategies have negligible effects on energy flexibility.



**Figure 33.** Dual-channel PV/T-PCM and heat pump system.

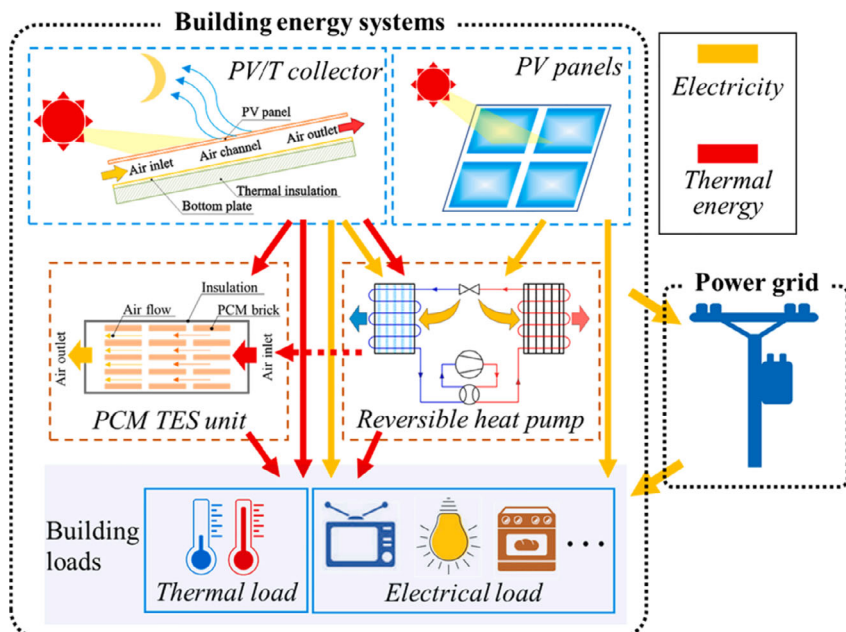


**Figure 34.** Schematic diagram of building energy system and energy flow.

**Table 11.** Summary of related studies on PV/T-PCM systems.

System types	PCMs	Highlights	Reference
Air-cooled PV/T-PCM system	Hydrated salt PCM 32/280	The performance of an air-cooled PV was investigated experimentally. Hydrated salt was used as PCM to increase the performance of cells. Four cases as natural convection and three forced convective were investigated. The investigation aims at utilizing the storage system in buildings. Using PCM results in reducing the cell temperature in the range of 3.7–4.3 °C.	[109]
Air-cooled PV/T-PCM system	CaCl <sub>2</sub> ·6H <sub>2</sub> O	The productivity of PCM integrated in PV/T air panels was evaluated through simulations using the optimized model. The simulation outcomes are pleasing and can be extended to other categories of panels where PCM can be positioned.	[110]
Air-cooled PV/T-PCM system	Not mentioned	The optimum thickness of PCM is found 77.2 mm. The annual CO <sub>2</sub> reduction is enhanced by 17.69% compared to using air (base case). 22.24% and 9.93% higher annual energy storage and electricity production are seen. Levelized cost is 11.959 cents kWh <sup>-1</sup> , which shows 9.59% improvement. The optimum condition enjoys payback period of 3.321 years.	[111]
Water-cooled PV/T-PCM system	Paraffin-coated MPCM	A study was conducted on the overall efficiency of a PV/T-MPCM system that utilizes water-cooling. A comparison was made between the electrical efficiency and thermal efficiency of a PV/T-MPCM system with water-cooling, using MPCM grout and tap water, under various operating conditions. A comparison was made between the real-life performance of a conventional water-cooled PV/T system and a similar system incorporating a PCM layer.	[112]
Water-cooled PV/T-PCM system	Paraffin	Various passive and active cooling PV/T systems were investigated, experimentally. Wide range (regular-concentrated) of solar radiation power (800–1700 Wm <sup>-2</sup> ) on PV/T was implemented. PCM was unfiltered in a special heat conductive foam (PS-CNT foam), as PCM-composite. PCM-composite can diminish the PV cell temperature up to 6.8% and increase electrical efficiency up to 14%. Energy efficiencies of the best PV/T examined in this investigation in passive and active cooling are 13–14.2% and 66.8–82.6%.	[113]
Water-cooled PV/T-PCM system	Paraffin+0.009 wt% functionalized CNT	Experimental investigation of NePCM-based PV/T. Latent heat capacity of PCM is fairly enhanced by the insertion of functionalized CNT. PV/T-NePCM system reduces cell temperature 4 °C more than PV/T-PCM system. PV/T-NePCM system raises water outlet temperature by more than 46 °C. Maximum overall energy and exergy efficiency are 85.3% and 12%, respectively.	[114]
Water-cooled PV/T-PCM system	Paraffin + 2.5 wt% Nano-CuO	Corrugated absorber was used in the bases of trays solar still. Wick was investigated on CTSS performance. Using internal mirrors, nanoenhanced PCM and PV-powered heaters were tested. The modifications improved the daily distillate of CTSS by 180% over the CSS.	[115]
Water-cooled PV/T-PCM system	Paraffin	A hybrid BIPV/T system with double-air channel and PCM is introduced. Seasonal energy demands of building both in day and night are satisfied. Room temperature is 0.6 °C lower/0.7 °C higher in day/night than reference room in transition. Room temperature is 10.8 °C higher/1.4 °C higher in day/night than reference room in winter. Room temperature is 1.2 °C lower/0.5 °C lower in day/night than reference room in summer.	[116]
Water-cooled PV/T-PCM system	Not mentioned	Dual-air channel and PCM are combined in this solar wall system. Mathematical model of this system is established and validated. Annual performance analyses are investigated in Urumqi, Beijing, and Hefei. Annual energies saved in the three cities are 863.24, 770.53, and 576.43 kWh. Impacts of some parameters on the annual performance are discussed and analyzed.	[117]
Water-cooled PV/T-PCM system	Paraffin+nano-Al <sub>2</sub> O <sub>3</sub>	The electrical efficiency of the CPV-T system varies between 10.82% and 11.32%. Drying rate was calculated to be 0.436 g matter g <sup>-1</sup> dry matter.min <sup>-1</sup> for this system. Overall thermal and exergy efficiency were found to be 20% and 8%, respectively. Prediction results of ANN and SVM algorithms were compared with four metrics. It is noticed that ANN and SVM have the ability to successfully predict the drying parameters.	[118]

**Table 11.** Continued.

System types	PCMs	Highlights	Reference
Water-cooled PV/T-PCM system	Paraffin	A compound parabolic CPV/T system integrated with PCM was constructed. The application of PCM improved the nonuniformity of temperature distribution.	[119]
Water-cooled PV/T-PCM system	Paraffin	The instantaneous and averaged primary energy efficiencies were calculated. A predictive model was developed based on the response surface method. Both single and multi-objective optimizations were conducted using RSM. The predicted responses for all goals are in the desirable range. The sensitivity of solar radiation is more than other operating factors.	[120]
Water-cooled PV/T-PCM system	Paraffin	The PV/T modules assembled with PCMs were numerically analyzed. The assembled PV/T structures were evaluated from the energetic and exergetic views. Embedding PCMs in PV/T modules are benefit for the CO <sub>2</sub> mitigation.	[121]
Nanofluid PV/T-PCM system	Paraffin	A SPV-THC was fabricated. Thermodynamic analysis of SPV-THC using CuO nanofluid was carried out. Thermal modeling for SPV-THC was developed and validated with experimental results. Performance of SPV-THC is better compared to opaque PV/T collector. Energy and exergy efficiency of CuO-based SPV-THC is higher than water-based system.	[122]
Nanofluid PV/T-PCM system	Paraffin	The thermoelectric performance of the system was evaluated using a validated and simulated comprehensive numerical model, considering both passive and active cooling conditions. The melting and solidification process of PCM under CR5 was studied. Passive cooling effectively keeps the temperature of CPV below 78 °C. Furthermore, with the implementation of active cooling, the PV cell's temperature is effectively regulated to remain below 43 °C, ensuring a consistent distribution throughout. The enhanced thermal conductivity and natural convection of the nanofluids within the PCM container are the primary factors contributing to this performance improvement.	[123]
Nanofluid PV/T-PCM system	Paraffin+nano-Al <sub>2</sub> O <sub>3</sub>	The performance of the collector was assessed by examining the impacts of varying mass flow rates and the inclusion of Al <sub>2</sub> O <sub>3</sub> nanoparticles in both the cooling water and PCM. A transient solver was selected to model the PV/T-LFR system. CFD method was used to solve the governing equation of PV/T-LFR. A basic algorithm was employed to connect velocity and pressure.	[124]
PV/T-PCM system with heat pump	Paraffin	A new hybrid heat pump system has been developed to provide a sustainable heating load. A novel PV/T panel and latent heat storage unit were designed for the heat pump system. The average COP value of hybrid heat pump system was obtained as 3.18. The average electrical efficiency of the PV/T was measured as 16.74%.	[125]
PV/T-PCM system with heat pump	Not mentioned	Paraffin in the latent heat storage unit could store thermal energy in 183 min. Using solar energy, thermal energy storage and demand-side management was studied. Improvement of energy flexibility was achieved solely by demand-side management. Thermal energy storage and demand-side management facilitated further improvement.	[126]

#### 4.5. Economy of PV/T-PCM Systems

The relevant studies of PV/T-PCM system are summarized in Table 11. As described in Section 3 of this article, PV/T-PCM systems are superior to PV-PCM systems in terms of energy efficiency. The trade-off, however, is higher input costs. The way to improve the economic benefit of PV/T-PCM system should be considered from these two perspectives: one is to reduce the system input cost, the other is to improve the energy efficiency by improving the system performance. Both are equally critical and therefore worth further study in the future. In addition, combined with energy saving, environmental protection, and economy, it is

necessary to establish an assessment standard to comprehensively evaluate the performance of PV/T-PCM systems, which is also worth the attention of researchers and energy managers.

#### 5. Conclusions and Perspectives for Future Research

##### 5.1. Conclusions

This article summarizes the research of PCMs integration in PV systems and PV/T systems. First, PCMs and LHTS technology

are introduced, and the classification, performance test, and composite modification methods of PCMs are summarized. Second, the relevant researches of PCMs in PV thermal management are summarized; the characteristics of PV-PCM, CPV-PCM, BIPV-PCM, and PV-TE-PCM systems are introduced in detail, and the representative researches in the past 20 years are cited based on research ideas. The feasibility and economic analysis of PV-PCM system are summarized, and the analysis is of great significance to the research and development of PV/T-PCM system. Lastly, this article continues to introduce and summarize the PV/T-PCM system in detail. The main conclusions of the literature survey are as follows. 1) the integration of PCMs and PV focuses on the preparation of PCMs with suitable phase-change temperature and good heat storage performance. To achieve the effect of PV thermal management, the optimal phase-change temperature range of PCMs is 25–35 °C, and the phase-change temperature should be as close to 25 °C as possible under the premise of ensuring the high latent heat and high thermal conductivity of PCMs. To find PCMs that meet the operating temperature, in addition to using pure materials with suitable phase-change temperature (such as paraffin,  $\text{CaCl}_2\text{H}_2\text{O}$ , etc.), suitable eutectic PCMs can also be found. Whether organic, inorganic or eutectic PCMs, their thermal conductivity has a certain gap from the PV thermal management requirements. If not modified to improve thermal conductivity, PCMs not only play a role in thermal management, but may also become an obstacle to the heat dissipation of PV cells. To improve the thermal conductivity of PCMs, an appropriate amount of thermal conductivity enhancer can be added to PCMs. Among them, the 0D structure additive nanoparticles can not only enhance the thermal conductivity function, but also reduce or even eliminate the supercooling degree of PCMs. Therefore, nanoparticles are favored by more researchers. To ensure the recycling of PCMs, the researchers began to focus on the solidification process of PCMs rather than just the melting process. Supercooling and phase separation may occur in the solidification process of inorganic PCMs. Adding suitable nucleating agent can reduce the supercooling degree of PCMs, adding suitable thickener or using porous material adsorption can solve the phase separation problem to a certain extent. Since the addition of additives will reduce the latent heat of PCMs, from this point of view, it may also make the thermal management ability of PCMs worse, so the use of additives is limited, not more is better. 2) The thermal management research of PCMs for PV cells includes PV-PCM systems, CPV-PCM systems, BIPV-PCM systems, and PV-TE-PCM systems. The research of PV thermal management based on PCMs began with PV-PCM systems, and after nearly 20 years of development, from aluminum model simulation or experiment with analog PV cells, to the improvement of the heat transfer structure of real PV cells and PCMs. In addition to the development of PCMs and the optimization of the heat transfer structure of PV-PCM systems, researchers have also paid attention to the influence of some internal and external factors, such as climatic conditions, PV cell inclination, and various environmental conditions, on the electrical efficiency of PV-PCM system. For the CPV-PCM systems, it is necessary to further improve the thermal conductivity of PCMs and design an efficient heat transfer and heat dissipation structure to meet the higher thermal management requirements brought about by the increase in temperature of PV cells caused

by CPV. The research of BIPV-PCM systems not only includes the development of PCMs, the study of the heat transfer structure of PCMs and PV cells, but also the introduction of PCMs is very important for the influence of PV building on comfort and energy saving. The PV-TE-PCM systems combine the TE generators with the PV-PCM systems to enhance the performance of the TE generators and the PV cells, achieving a win-win situation. Through the feasibility and economic analysis of PV-PCM systems, it can be seen that the use of heat energy collected by PCMs in PV-PCM systems can effectively shorten the recovery period of PV-PCM systems, and PV/T-PCM systems came into being. 3) Because the research of PV-PCM systems has a certain foundation, although the PV/T-PCM systems started late, their development is fast in recent years. PV/T-PCM systems can be divided into air-cooled PV/T-PCM systems, water-cooled PV/T-PCM systems and nanofluid PV/T-PCM systems. Since the thermal conductivity of water is greater than that of air and ethylene glycol, the research of water-cooled PV/T-PCM systems has become the mainstream. The current research focus of water-cooled PV/T-PCM system can be summarized into three aspects: in the PCMs development, the research focus is on packaging and nanoparticles enhanced thermal conductivity; applications include water-cooled CPV/T-PCM systems and water-cooled BIPV/T-PCM systems; heat transfer structure optimization is no longer limited to the use of fins, and began to use theoretical research methods such as RSM to optimize. The heat energy collected by water-cooled PV/T-PCM systems is very limited, and the water temperature after the cooling water passes through the PCMs can only barely meet the domestic water demand, and the thermal efficiency of the water-cooled PV/T-PCM systems needs to be improved. Using nanofluids instead of cooling water as the coolant can improve both the electrical and thermal efficiency of the PV/T-PCM systems, while the combination of the PV/T-PCM system with a heat pump can significantly increase the heat collection temperature.

## 5.2. Perspectives for Future Research

In the past 20 years, researchers have paid great attention to PCMs integration in PV and PV/T, and have achieved many meaningful research results. However, there are still shortcomings in the past studies, which are summarized in **Table 12**. In the context of double carbon, there are some new research ideas worth learning from researchers. Suggestions for future developments in this area are summarized as follows. 1) At present, the means to improve the thermal conductivity of PCMs is focused on the PCMs itself, that is, the use of thermal conductivity enhancer to improve the thermal conductivity of PCMs. The degree of adhesion between PCMs and heat transfer structure determines the contact thermal resistance. The use of flexible PCMs can increase the degree of adhesion between PCMs and heat transfer structure to reduce the contact thermal resistance, which has been applied to the thermal management of power batteries. But many studies on PV cells and PCMs have not paid attention to this point. At present, the optimization of heat transfer structure of PV-PCM and PV/T-PCM systems is mostly experimental, and few studies have been advanced to the theoretical level. In the future, more theoretical research

**Table 12.** Research gaps on PV and PV/T technologies of integrated PCMs.

Research gaps on PV and PV/T technologies of integrated PCMs.
There is no research on reducing the contact thermal resistance between PCM and heat transfer structure in the system.
The optimization of heat transfer structure of PV-PCM and PV/T-PCM systems is mostly experimental, and few studies have been advanced to the theoretical level.
The PCM scheme suitable for the PV system in the whole year condition needs to be proposed.
The PCMs' optimization criteria of PV and CPV need to be summarized by researchers using mathematical statistics and other methods.
The performance of PV-PCM and PV/T-PCM systems is still mainly based on electrical efficiency and thermal efficiency, and few papers rise to exergy and entransy dissipation.
Energy efficiency and CO <sub>2</sub> emission reduction should be generally considered in the performance of BIPV-PCM and BIPV/T-PCM systems.
The difference of influence of nanomaterials on cooling water and PCMs should be analyzed from the mechanism.
The design and research of new control strategies for PV/T-PCM systems deserve the attention of engineers and researchers in the future.
From the perspective of whole life cycle management, it is necessary to establish an evaluation standard to comprehensively evaluate the performance of PV/T-PCM systems by means of combining energy saving, environmental protection and economy.

ideas and methods such as GA, BP neural network, and big data can be applied to obtain the optimal shape, size, and quantity of heat transfer structures. 2) Given that the climate throughout the year varies with the seasons, the large temperature difference between summer and winter means that a scheme using only one type of PCM may not be suitable for the whole year. Therefore, the PCM scheme suitable for the PV system in the whole year condition needs to be proposed. In this regard, it may be possible to design a two-stage thermal management PV-PCM system by combining two PCMs with different phase-change temperatures. Stabilizing supercooled PCM may also be a good attempt. 3) The effect of PCMs is also related to the latent heat value, an important performance parameter, and most of the additives will reduce the latent heat of PCMs to a certain extent. The addition of additives should not only look at the improvement effect of a certain parameter, but should comprehensively consider all important thermal property parameters. The PCMs' optimization criteria of PV and CPV need to be summarized by researchers using mathematical statistics and other methods. 4) The performance of PV-PCM and PV/T-PCM systems is still mainly based on electrical efficiency and thermal efficiency, and few papers rise to exergy and entransy dissipation, which should be taken into account in future studies. Energy efficiency and CO<sub>2</sub> emission reduction should be generally considered in the performance of BIPV-PCM and BIPV/T-PCM systems. 5) The significant improvement of the TE performance of the PV/T-PCM systems by nanofluids is noteworthy, and the flow simulation and experimental study of the nanofluids and NePCMs units at micro- and macrolevels are worth carrying out. The difference of influence of nanomaterials on cooling

water and PCMs should be analyzed from the mechanism. 6) To further optimize the temperature uniformity of PV cells in PV/T-PCM systems and realize the high efficiency and reasonable cogeneration, the design and research of new control strategies for PV/T-PCM systems deserve the attention of engineers and researchers in the future. 7) PV/T-PCM systems increase the cost while increasing the energy efficiency, so the economy of PV/T-PCM systems deserves attention to reduce the cost or improve the energy efficiency, deciding the ideal way improving the economy of PV/T-PCM systems more effectively. From the perspective of whole life cycle management, it is necessary to establish an evaluation standard to comprehensively evaluate the performance of PV/T-PCM systems by means of combining energy saving, environmental protection, and economy.

## Acknowledgements

This work was funded by the project of Shanghai Science and Technology Commission (grant no. 19DZ1203102).

## Conflict of Interest

The authors declare no conflict of interest.

## Keywords

heat exchanges, integration of heat and power generations, phase-change materials (PCMs), photovoltaics (PVs), thermal managements

Received: January 14, 2024

Revised: February 18, 2024

Published online: March 18, 2024

- [1] R. Kumar, A. K. Pandey, M. Samykano, B. Aljafari, Z. Ma, S. Bhattacharya, V. Goel, I. Ali, R. Kothari, V. V. Tyagi, *Renewable Sustainable Energy Rev.* **2022**, 165, 112611.
- [2] H. M. Ali, *J. Build. Eng.* **2022**, 56, 104731.
- [3] L. Zou, Y. Liu, J. Yu, *Renewable Energy* **2023**, 217, 119119.
- [4] V. K. Raj, V. Baiju, F. P. Junaid, *J. Energy Storage* **2022**, 45, 103696.
- [5] X. Zhang, Y. Zhang, H. Li, Z. Chen, *Sol. Energy Mater. Sol. Cells* **2023**, 256, 112336.
- [6] V. Baiju, *Appl. Energy* **2023**, 351, 121825.
- [7] B. M. Tripathi, S. K. Shukla, P. K. S. Rathore, *J. Energy Storage* **2023**, 72, 108280.
- [8] M. Mehrali, J. E. ten Elshof, M. Shahi, A. Mahmoudi, *Chem. Eng. J.* **2021**, 405, 126624.
- [9] H. Hu, H. Zhang, S. Hong, *Mater. Lett.* **2023**, 352, 135166.
- [10] Y. Chen, H. He, J. Li, H. He, S. Chen, C. Deng, *Mater. Lett.* **2023**, 342, 134320.
- [11] M. Sivashankar, C. Selvam, *J. Energy Storage* **2022**, 55, 105575.
- [12] F. Hachem, B. Abdulhay, M. Ramadan, H. E. Hage, M. G. E. Rab, M. Khaled, *Renewable Energy* **2017**, 107, 567.
- [13] M. K. Sharma, *J. Energy Storage* **2022**, 48, 104020.
- [14] Y. Xiao, P. Huang, G. Wei, L. Cui, C. Xu, X. Du, *J. Energy Storage* **2022**, 56, 106073.
- [15] N. Soares, J. J. Costa, A. R. Gaspar, P. Santos, *Energy Build.* **2013**, 59, 82.
- [16] M. H. Zahir, K. Irshad, M. Shafiullah, N. I. Ibrahim, A. K. M. K. Islam, K. O. Mohaisen, F. A. A. Sulaiman, *J. Energy Storage* **2023**, 64, 107156.

- [17] T. Yang, Y. Ding, B. Li, A. K. Athienitis, *Build. Environ.* **2023**, 244, 110711.
- [18] M. Chen, Y. He, Q. Ye, Z. Zhang, Y. Hu, *Int. J. Heat Mass Transfer* **2019**, 130, 1133.
- [19] F. Jamil, F. Hassan, S. Shoeibi, M. Khiadani, *Renewable Sustainable Energy Rev.* **2023**, 186, 113663.
- [20] V. Goel, A. Saxena, M. Kumar, A. Thakur, A. Sharma, V. Bianco, *Appl. Therm. Eng.* **2023**, 219, 119417.
- [21] F. Gao, X. Wang, D. Wu, *Sol. Energy Mater. Sol. Cells* **2017**, 168, 146.
- [22] X. Wang, W. Li, Z. Luo, K. Wang, S. P. Shah, *Energy Build.* **2022**, 260, 111923.
- [23] Y. Zhang, Y. Jiang, Y. Jiang, *Meas. Sci. Technol.* **1999**, 10, 201.
- [24] A. Solé, L. Miró, C. Barreneche, I. Martorell, L. F. Cabeza, *Renewable Sustainable Energy Rev.* **2013**, 26, 425.
- [25] C. Xu, H. Zhang, G. Fang, *J. Energy Storage* **2022**, 51, 104568.
- [26] D. Vitiello, B. Nait-Ali, N. Tessier-Doyen, T. Tonnesen, L. Laíñ, L. Rebouillat, D. S. Smith, *Open Ceram.* **2021**, 6, 100118.
- [27] W. Zhao, Y. Yang, Z. Bao, D. Yan, Z. Zhu, *Int. J. Hydrogen Energy* **2020**, 45, 6680.
- [28] I. Asadi, P. Shafiq, Z. F. B. A. Hassan, N. B. Mahyuddin, *J. Build. Eng.* **2018**, 20, 81.
- [29] S. Sun, X. Jin, C. Liu, Q. Meng, Y. Zhang, *Int. J. Heat Mass Transfer* **2018**, 127, 88.
- [30] Y. H. Park, D. Y. Ku, M. Y. Ahn, Y. Lee, S. Cho, *Fusion Eng. Des.* **2019**, 146, 950.
- [31] B. Liu, X. Zhang, J. Ji, W. Hua, F. Mao, *Int. J. Energy Res.* **2020**, 44, 3626.
- [32] P. Singh, R. K. Sharma, G. Hekimoğlu, A. Sari, O. Gencel, V. V. Tyagi, *J. Energy Storage* **2023**, 64, 107205.
- [33] A. M. Oliveira, A. P. Oliveira, J. D. Vieira, A. N. Junior, O. Cascudo, *J. Build. Eng.* **2023**, 64, 105616.
- [34] Q. Yao, J. Guo, Y. Liu, F. Guan, S. Liu, X. Huang, X. Zhang, Q. Yang, *J. Energy Storage* **2023**, 71, 108164.
- [35] X. Man, H. Lu, Q. Xu, C. Wang, Z. Ling, *J. Energy Storage* **2023**, 72, 108699.
- [36] P. Dixit, V. J. Reddy, S. Parvate, A. Balwani, J. Singh, T. K. Maiti, A. Dasari, S. Chattopadhyay, *J. Energy Storage* **2022**, 51, 104360.
- [37] T. Xu, X. Tang, J. Wang, M. Li, J. Li, J. Yang, Y. Bie, *Appl. Therm. Eng.* **2022**, 210, 118370.
- [38] Q. Wang, J. Wang, Y. Chen, C. Y. Zhao, *Sol. Energy* **2019**, 177, 99.
- [39] G. R. Dheep, A. Sreekumar, *Energy Convers. Manage.* **2014**, 83, 133.
- [40] Z. Chen, X. Zhang, J. Ji, Y. Lv, *J. Energy Storage* **2022**, 56, 106157.
- [41] M. Sun, T. Liu, H. Sha, M. Li, T. Liu, X. Wang, G. Chen, J. Wang, D. Jiang, *J. Energy Storage* **2023**, 68, 107713.
- [42] H. Wang, E. Ci, X. Li, Y. Zhang, Z. Zhang, J. Li, *J. Energy Storage* **2022**, 48, 103979.
- [43] B. Kalidasan, A. K. Pandey, R. Saidur, R. Kothari, K. Sharma, V. V. Tyagi, *Sol. Energy Mater. Sol. Cells* **2023**, 262, 112534.
- [44] T. Liao, F. Luo, X. Liang, S. Wang, X. Gao, Z. Zhang, Y. Fang, *J. Energy Storage* **2023**, 59, 106495.
- [45] G. Sang, H. Zeng, Z. Guo, H. Cui, Y. Zhang, X. Cui, L. Zhang, W. Han, *J. Build. Eng.* **2022**, 59, 105010.
- [46] R. Luque, A. Ahmad, S. Tariq, M. Mubashir, M. S. Javed, S. Rajendran, R. S. Varma, A. Ali, C. Xia, *Mater. Today* **2023**.
- [47] Y. Fang, K. Wang, Y. Ding, X. Liang, S. Wang, X. Gao, Z. Zhang, *Sol. Energy Mater. Sol. Cells* **2021**, 232, 111355.
- [48] H. Zhang, Q. Dong, Y. Tang, J. Wu, W. Bi, Y. Gao, J. Wang, H. Yang, *Chem. Eng. J.* **2023**, 471, 144462.
- [49] S. S. Hoseini, A. Seyedkanani, G. Najafi, A. P. Sasmito, A. Akbarzadeh, *Energy Storage Mater.* **2023**, 59, 102768.
- [50] S. Cai, X. Zhang, J. Ji, *J. Energy Storage* **2023**, 72, 108750.
- [51] W. Liu, X. Zhang, J. Ji, Y. Wu, L. Liu, *Energy Technol.* **2021**, 9, 2100169.
- [52] Y. A. Bhutto, A. K. Pandey, R. Saidur, K. Sharma, V. V. Tyagi, *Mater. Today Sustainability* **2023**, 23, 100443.
- [53] A. Mitra, R. Kumar, D. K. Singh, Z. Said, *J. Energy Storage* **2022**, 53, 105195.
- [54] S. Tan, X. Zhang, *J. Energy Storage* **2023**, 61, 106772.
- [55] C. Ding, C. Shao, S. Wu, Y. Ma, Y. Liu, S. Ma, X. Hu, Z. Cao, X. Ren, B. Zhong, G. Wen, X. Huang, *Carbon* **2023**, 213, 118279.
- [56] K. Ghasemi, S. Tasnim, S. Mahmud, *Sustainable Energy Technol. Assess.* **2022**, 52, 102084.
- [57] B. K. Choure, T. Alam, R. Kumar, *J. Energy Storage* **2023**, 72, 108161.
- [58] X. Yang, C. Li, Y. Ma, H. Chi, Z. Hu, J. Xie, *Chem. Eng. J.* **2023**, 473, 145364.
- [59] M. Deng, C. Zhao, J. Li, N. Sheng, C. Zhu, Z. Rao, *Ceram. Int.* **2023**, 49, 31175.
- [60] J. Weng, Q. Huang, X. Li, G. Zhang, D. Ouyang, M. Chen, A. C. Yuen, A. Li, E. W. M. Lee, W. Yang, J. Wang, X. Yang, *Energy Storage Mater.* **2022**, 53, 580.
- [61] R. Arivazhagan, N. B. Geetha, R. Pandiyarajan, *J. Eng. Res.* **2023**.
- [62] M. Mohseni, A. H. Novin, *J. Syst. Archit.* **2023**, 144, 103008.
- [63] A. Waqas, J. Ji, L. Xu, M. Ali, . Zeashan, J. Alvi, *Renewable Sustainable Energy Rev.* **2018**, 92, 254.
- [64] L. Gao, X. Zhang, W. Hua, *J. Energy Storage* **2023**, 65, 107317.
- [65] S. Preet, *Clim. Change* **2021**, 2, 100033.
- [66] R. M. Elavarasan, V. Mudgal, L. Selvamanohar, K. Wang, G. Huang, G. M. Shafullah, C. N. Markides, K. S. Reddy, M. Nadarajah, *Energy Convers. Manage.* **2022**, 255, 115278.
- [67] A. A. Miaari, H. M. Ali, *Case Stud. Therm. Eng.* **2023**, 49, 103283.
- [68] S. Preet, *Renewable Sustainable Energy Rev.* **2018**, 82, 791.
- [69] T. Wongwuttanasatian, T. Sarikarin, A. Suksri, *Sol. Energy* **2020**, 195, 47.
- [70] M. J. Huang, P. C. Eames, B. Norton, *Int. J. Heat Mass Transfer* **2004**, 47, 2715.
- [71] M. J. Huang, P. C. Eames, B. Norton, N. J. Hewitt, *Sol. Energy Mater. Sol. Cells* **2011**, 95, 1598.
- [72] C. J. Smith, P. M. Forster, R. Crook, *Appl. Energy* **2014**, 126, 21.
- [73] S. Khanna, K. S. Reddy, T. K. Mallick, *Energy Convers. Manage.* **2018**, 166, 590.
- [74] S. Foteinis, N. Savvakis, T. Tsoutsos, *Energy* **2023**, 265, 126355.
- [75] M. Rezvanpour, D. Borooghani, F. Torabi, M. Pazoki, *Renewable Energy* **2020**, 146, 1907.
- [76] Y. Zhang, X. Zhang, *Sol. Energy* **2020**, 204, 683.
- [77] B. Karami, N. Azimi, S. Ahmadi, *Renewable Energy* **2021**, 178, 25.
- [78] X. Li, J. Duan, T. Simon, T. Ma, T. Cui, Q. Wang, *Appl. Energy* **2021**, 298, 117203.
- [79] X. Li, W. Cui, T. Simon, T. Ma, T. Cui, Q. Wang, *Appl. Energy* **2021**, 302, 117558.
- [80] J. Feng, J. Huang, Z. Ling, X. Fang, Z. Zhang, *Sol. Energy Mater. Sol. Cells* **2021**, 225, 111060.
- [81] S. Khanna, K. S. Reddy, T. K. Mallick, *Int. J. Therm. Sci.* **2018**, 130, 313.
- [82] S. Khanna, S. Newar, V. Sharma, K. S. Reddy, T. K. Mallick, *Energy Convers. Manage.* **2019**, 180, 1185.
- [83] P. Singh, S. Khanna, V. Becerra, S. Newar, V. Sharma, T. K. Mallick, D. Hutchinson, J. Radulovic, R. Khusainov, *Energy* **2020**, 193, 116735.
- [84] A. Akshayveer, *J. Energy Storage* **2022**, 46, 103814.
- [85] S. Khanna, P. Singh, V. Mudgal, S. Newar, V. Sharma, V. Becerra, K. S. Reddy, T. K. Mallick, *Energy* **2022**, 243, 122923.
- [86] M. Shoaib, S. Y. Khan, N. Ahmed, M. Mahmood, A. Waqas, M. A. Qaisrani, N. Shehzad, *J. Energy Storage* **2022**, 52, 104956.
- [87] S. Khanna, K. S. Reddy, T. K. Mallick, *Energy* **2017**, 133, 887.
- [88] N. Variji, M. Siavashi, M. Tahmasbi, M. Bidabadi, *J. Energy Storage* **2022**, 50, 104690.
- [89] M. Nouira, H. Sammouda, *Appl. Therm. Eng.* **2018**, 141, 958.

- [90] S. Khanna, S. Newar, V. Sharma, K. S. Reddy, T. K. Mallick, J. Radulovic, R. Khusainov, D. Hutchinson, V. Becerra, *J. Cleaner Prod.* **2019**, 221, 878.
- [91] S. Adibpour, A. Raisi, B. Ghasemi, A. R. Sajadi, G. Rosengarten, *Renewable Energy* **2021**, 165, 321.
- [92] A. Chibani, S. Merouani, H. Laidoudi, A. Dehane, M. R. Morakchi, L. Bendada, *J. Energy Storage* **2023**, 72, 108283.
- [93] I. Zarma, M. Ahmed, S. Ookawara, *Energy Convers. Manage.* **2019**, 179, 229.
- [94] M. Sivashankar, C. Selvam, S. Manikandan, S. Harish, *Energy* **2020**, 208, 118408.
- [95] M. Emam, M. Ahmed, *Energy Convers. Manage.* **2018**, 158, 298.
- [96] S. Manikandan, C. Selvam, N. Poddar, K. Pranjyal, R. Lamba, S. C. Kaushik, *J. Cleaner Prod.* **2019**, 219, 359.
- [97] M. M. Elsabahy, M. Ahmed, H. Sekiguchi, M. Emam, *Energy Convers. Manage.* **2022**, 266, 115854.
- [98] E. Asadi, M. G. da Silva, C. H. Antunes, L. Dias, *Energy Build.* **2012**, 44, 81.
- [99] D. Singh, A. K. Gautam, R. Chaudhary, *Mater. Today: Proc.* **2021**, 45, 4624.
- [100] K. Kant, A. Anand, A. Shukla, A. Sharma, *J. Energy Storage* **2020**, 30, 101563.
- [101] A. Karthick, K. K. Murugavel, A. Ghosh, K. Sudhakar, P. Ramanan, *Sol. Energy Mater. Sol. Cells* **2020**, 207, 110360.
- [102] A. Karthick, K. K. Murugavel, P. Ramanan, *Energy* **2018**, 142, 803.
- [103] X. Sun, Y. Lin, Z. Zhu, J. Li, *Appl. Energy* **2022**, 306, 118010.
- [104] H. H. Jo, Y. Kang, S. Yang, Y. U. Kim, B. Y. Yun, J. D. Chang, S. Kim, *Renewable Energy* **2022**, 195, 1412.
- [105] H. Metwally, N. A. Mahmoud, M. Ezzat, W. Aboelsoud, *J. Energy Storage* **2021**, 42, 103031.
- [106] A. Yusuf, S. Ballikaya, *J. Energy Storage* **2023**, 59, 106544.
- [107] J. Zhao, T. Ma, Z. Li, A. Song, *Appl. Energy* **2019**, 245, 51.
- [108] Y. Gao, D. Wu, Z. Dai, C. Wang, B. Chen, X. Zhang, *Renewable Energy* **2023**, 207, 539.
- [109] N. Choubineh, H. Jannesari, A. Kasaeian, *Renewable Sustainable Energy Rev.* **2019**, 101, 103.
- [110] I. Kanzari, H. Oueslati, S. B. Mabrouk, *Renewable Energy Focus* **2021**, 37, 27.
- [111] A. Sohani, A. Dehnavi, H. Sayyaadi, S. Hoseinzadeh, E. Goodarzi, D. A. Garcia, D. Groppi, *J. Energy Storage* **2022**, 46, 103777.
- [112] Z. Fu, Y. Li, X. Liang, S. Lou, Z. Qiu, Z. Cheng, Q. Zhu, *Energy* **2021**, 228, 120509.
- [113] R. Ahmadi, F. Monadinia, M. Maleki, *Sol. Energy Mater. Sol. Cells* **2021**, 222, 110942.
- [114] M. M. Islam, M. Hasanuzzaman, N. A. Rahim, A. K. Pandey, M. Rawa, L. Kumar, *Renewable Energy* **2021**, 172, 71.
- [115] A. S. Abdullah, Z. M. Omara, F. A. Essa, M. M. Younes, S. Shanmugan, M. Abdelgaied, M. I. Amro, A. E. Kabeel, W. M. Farouk, *J. Energy Storage* **2021**, 40, 102782.
- [116] L. Xu, J. Ji, J. Cai, W. Ke, X. Tian, B. Yu, J. Wang, *Renewable Energy* **2021**, 173, 596.
- [117] W. Ke, J. Ji, L. Xu, H. Xie, C. Wang, B. Yu, *Energy* **2021**, 235, 121359.
- [118] M. O. Karaağaç, A. Ergün, Ü. Ağbulut, A. E. Gürel, İ. Ceylan, *Sol. Energy* **2021**, 218, 57.
- [119] X. Kong, L. Zhang, H. Li, Y. Wang, M. Fan, *Sol. Energy Mater. Sol. Cells* **2022**, 234, 111415.
- [120] A. Kazemian, Y. Basati, M. Khatibi, T. Ma, *J. Cleaner Prod.* **2021**, 290, 125748.
- [121] M. A. El-Hamid, G. Wei, L. Cui, C. Xu, X. Du, *Appl. Therm. Eng.* **2022**, 208, 118222.
- [122] P. Jidhesh, T. V. Arjunan, N. Gunasekar, *J. Cleaner Prod.* **2021**, 316, 128360.
- [123] S. Rahmanian, H. Rahmanian-Koushkaki, P. Omidvar, A. Shahsavar, *Sustainable Energy Technol. Assess.* **2021**, 46, 101223.
- [124] M. Khodadadi, S. A. Farshad, Z. Ebriahimpour, M. Sheikhholeslami, *Sustainable Energy Technol. Assess.* **2021**, 47, 101340.
- [125] M. Koşan, M. Aktaş, *Appl. Therm. Eng.* **2021**, 199, 117524.
- [126] H. Ren, Y. Sun, A. K. Albdoor, V. V. Tyagi, A. K. Pandey, Z. Ma, *Appl. Energy* **2021**, 285, 116433.
- [127] Y. Wang, J. Sui, Z. Xu, *Energy* **2022**, 259, 125036.
- [128] C. Li, B. Zhang, B. Xie, X. Zhao, J. Chen, *Energy Convers. Manage.* **2020**, 208, 112586.
- [129] N. Kumar, D. Banerjee, R. Chavez, *J. Energy Storage* **2018**, 20, 153.
- [130] N. Xie, X. Gao, Y. Zhong, R. Ye, S. Chen, L. Ding, T. Zhong, *J. Build. Eng.* **2022**, 56, 104747.
- [131] Q. Xiao, J. Fan, Y. Fang, L. Li, T. Xu, W. Yuan, *Appl. Therm. Eng.* **2018**, 136, 701.
- [132] Q. Xiao, W. Yuan, L. Li, Tao Xu, *Sol. Energy Mater. Sol. Cells* **2018**, 179, 339.
- [133] N. Gupta, A. Kumar, H. Dhasmana, V. Kumar, A. Kumar, P. Shukla, A. Verma, G. V. Nutan, S. K. Dhawan, V. K. Jain, *J. Energy Storage* **2020**, 32, 101773.
- [134] F. Mao, X. Zhang, Y. Zhang, B. Liu, L. Zheng, *J. Appl. Polym. Sci.* **2022**, 139, 51422.
- [135] Z. Song, Y. Deng, J. Li, H. Nian, *Mater. Res. Bull.* **2018**, 102, 203.
- [136] C. Li, M. Li, Y. Li, J. *Energy Storage* **2022**, 56, 105798.
- [137] J. Wang, Y. Yin, Y. Wang, J. Huang, *Appl. Therm. Eng.* **2023**, 219, 119666.
- [138] L. Que, X. Zhang, *J. Energy Storage* **2022**, 54, 105360.
- [139] N. Gupta, A. Kumar, H. Dhasmana, A. Kumar, A. Verma, P. Shukla, V. K. Jain, *J. Energy Storage* **2021**, 41, 102899.
- [140] J. Dai, R. Ling, K. Wang, *Adv. Mater. Res.* **2011**, 418, 282.
- [141] R. Pilar, L. Svoboda, P. Honcova, L. Oravova, *Thermochim. Acta* **2012**, 546, 81.
- [142] N. Gupta, A. Kumar, S. K. Dhawan, H. Dhasmana, A. Kumar, V. Kumar, A. Verma, V. K. Jain, *Mater. Today: Proc.* **2020**, 32, 463.
- [143] M. Pandya, A. K. Ansu, R. K. Sharma, *Mater. Today: Proc.* **2022**, 63, 786.
- [144] R. Wen, X. Zhu, C. Yang, Z. Sun, L. Zhang, Y. Xu, J. Qiao, X. Wu, X. Min, Z. Huang, *J. Energy Storage* **2022**, 46, 103921.
- [145] B. Tang, C. Wu, M. Qiu, X. Zhang, S. Zhang, *Mater. Chem. Phys.* **2014**, 144, 162.
- [146] Y. Tang, D. Su, X. Huang, G. Alva, L. Liu, G. Fang, *Appl. Energy* **2016**, 180, 116.
- [147] Y. Liu, Y. Yang, *Sol. Energy Mater. Sol. Cells* **2017**, 160, 18.
- [148] K. P. Venkitaraj, S. Suresh, B. Praveen, S. C. Nair, *J. Energy Storage* **2018**, 17, 1.
- [149] P. M. J. Stalin, Y. Naresh, T. Vamsi, K. Harivarma, G. V. Rao, J. Nagarjuna, *Mater. Today: Proc.* **2022**, 50, 1243.
- [150] P. M. J. Stalin, K. S. Prasad, K. P. Kumar, G. Hemadri, M. Rajesh, K. P. Kumar, *Mater. Today: Proc.* **2022**, 50, 1553.
- [151] S. Harikrishnan, M. Deenadhayalan, S. Kalaiselvam, *Energy Convers. Manage.* **2014**, 86, 864.
- [152] S. Sami, N. Etesami, *Appl. Therm. Eng.* **2017**, 124, 346.
- [153] F. Wang, W. Zheng, Y. Gou, Y. Jia, H. Li, J. *Energy Storage* **2022**, 53, 105077.
- [154] N. Şahan, M. Fois, H. Paksoy, *Sol. Energy Mater. Sol. Cells* **2015**, 137, 61.
- [155] P. V. Vineeth, K. D. Reddy, *Mater. Today: Proc.* **2023**.
- [156] P. M. Kumar, P. Chauhan, A. K. Sharma, M. L. Rinawa, A. J. Rahul, M. Srinivas, A. Tamilarasan, *Mater. Today: Proc.* **2022**, 62, 1894.
- [157] M. Amin, N. Putra, E. A. Kosasih, E. Prawiro, R. A. Luanto, T. M. I. Mahlia, *Appl. Therm. Eng.* **2017**, 112, 273.
- [158] B. Mu, Min Li, *Sci. Rep.* **2018**, 8, 8878.
- [159] J. Wang, H. Xie, Z. Xin, Y. Li, L. Chen, *Sol. Energy* **2010**, 84, 339.

- [160] A. Karaipekli, A. Biçer, A. Sarı, V. V. Tyagi, *Energy Convers. Manage.* **2017**, 134, 373.
- [161] X. Zhang, R. Wen, Z. Huang, C. Tang, Y. Huang, Y. Liu, M. Fang, X. Wu, X. Min, Y. Xu, *Energy Build.* **2017**, 149, 463.
- [162] C. Yang, M. E. Navarro, B. Zhao, G. Leng, G. Xu, L. Wang, Y. Jin, Y. Ding, *Sol. Energy Mater. Sol. Cells* **2016**, 152, 103.
- [163] X. Zhu, L. Han, F. Yang, J. Jiang, X. Jia, *Sol. Energy Mater. Sol. Cells* **2020**, 208, 110361.
- [164] C. Zhu, Y. Chen, R. Cong, F. Ran, G. Fang, *Sol. Energy Mater. Sol. Cells* **2021**, 219, 110782.
- [165] N. Zhang, Y. Song, Y. Du, Y. Yuan, G. Xiao, Y. Gui, *Adv. Eng. Mater.* **2018**, 20, 1800237.
- [166] G. Ma, J. Sun, Y. Zhang, Y. Jing, Y. Jia, *Powder Technol.* **2019**, 342, 131.
- [167] C. Chen, X. Liu, W. Liu, M. Ma, *Sol. Energy Mater. Sol. Cells* **2014**, 127, 14.



**Manting Fang** is a Ph.D. candidate of marine engineering at Shanghai Maritime University. His main research interest is the application of PV/T-PCM systems in ships. He published research on the application of PCMs in solar energy utilization.



**Xuelai Zhang** received his Ph.D. degree from the University of Shanghai for Science and Technology in 2000. He is a professor of power engineering and engineering thermo-physics at the Faculty of Shanghai Maritime University. His research interests include heat energy storage, cold chain transport, as well as the application of phase-change material in thermal management system.



**Yang Liu** studied power engineering and engineering thermo-physics at Shanghai Maritime University. She specializes in flexible phase-change materials and binary eutectic of materials.



**Shaowei Cai** is studying clean energy technology at Shanghai Maritime University, with a research focus on the application of phase-change materials in battery thermal management.